Explicit Multi-Symplectic Extended Leap-frog Methods for Hamiltonian Wave Equations

Wei Shi[a], Xinyuan Wu[a], Jianlin Xia[b,*]

[a]*Department of Mathematics, Nanjing University; State Key Laboratory for Novel Software Technology at Nanjing University, Nanjing 210093, P.R.China*
[b]*Department of Mathematics, Purdue University, West Lafayette, IN 47907, USA*

Abstract

In this paper, we study the integration of Hamiltonian wave equations whose solutions have oscillatory behaviors in time and/or space. We are mainly concerned with the research for multi-symplectic *extended Runge-Kutta-Nyström* (ERKN) discretizations and the corresponding discrete conservation laws. We first show that the discretizations to the Hamiltonian wave equations using two symplectic ERKN methods in space and time respectively lead to an explicit multi-symplectic integrator (Eleap-frogI). Then we derive another multi-symplectic discretization using a symplectic ERKN method in time and a symplectic Partitioned Runge-Kutta method, which is equivalent to the well-known Störmer-Verlet method in space (Eleap-frogII). These two new multi-symplectic schemes are extensions of the leap-frog method. The numerical stability and dispersive properties of the new schemes are analyzed. Numerical experiments with comparisons are presented, where the two new explicit multi-symplectic methods and the leap-frog method are applied to the linear wave equation and the sine-Gordon equation. The numerical results confirm the superior performance and some significant advantages of our new integrators in the sense of structure preservation.

Keywords: Multi-symplectic integrators, Hamiltonian wave equations, extended leap-frog methods, conservation laws, dispersive properties

Mathematics Subject Classification (2000): 35L05, 37M15, 65L06, 65M12, 65P10, 70S10

1. Introduction

It is well-known that symplectic integrators are robust, efficient, and accurate in preserving the long-time behavior of the solutions of Hamiltonian ordinary differential equations (ODEs) [1]. The basic idea of a symplectic integrator is that the numerical scheme is designed to preserve the symplectic form at each time step. Recently, it is shown that many conservative partial differential equations (PDEs), such as wave equations, generalized KdV and nonlinear Schrödinger equations, etc., allow for a structure similar to the symplectic structure of Hamiltonian ODEs, called the multi-symplectic formulation (see, e.g., [2, 3, 4]). For example, in [4], Marsden and Shkoller develop the multi-symplectic structure of Hamiltonian PDEs from a Lagrangian formulation using a variational principle.

It is natural to design integrators for Hamiltonian PDEs which preserve a semi-discretization of the symplectic form associated with the infinite-dimensional evolution equation. In the past decade, rapid progress

☆The research of Wei Shi and Xinyuan Wu was supported in part by the Natural Science Foundation of China under Grant 10771099 and by the Specialized Research Foundation for the Doctoral Program of Higher Education under Grant 20100091110033, by the 985 Project at Nanjing University under Grant 9112020301, by A Project Founded by the Priority Academic Program Development of Jiangsu Higher Education Institutions, and by the University Postgraduate Research and Innovation Project of Jiangsu Province 2012 under Grant CXLX12_0033.

☆☆The research of Jianlin Xia was supported in part by NSF grants DMS-1115572 and CHE-0957024.

*Corresponding author.

Email address: shuier628@163.com, xywu@nju.edu.cn, xiaj@math.purdue.edu (Jianlin Xia)

has been made on the development of *multi-symplectic integrators* of Runge-Kutta type for various Hamiltonian PDEs (see, e.g., [5, 6, 7, 8, 9, 10, 11, 12]). Unfortunately, most of the existing multi-symplectic integrators fail to take into account the oscillatory behavior of the problems of interest, which is important for the solution that has the intrinsic oscillatory behavior.

It is known that most of integrators adapted to the oscillatory problems are frequency-dependent, such as ARKN methods [13, 14, 15, 16, 17], ERKN methods [18, 19, 20, 21], and trigonometrically/exponentially-fitted methods [22, 23, 24, 25]. For nonlinear Schrödinger equations, taking the frequency of the problem into account, several useful trigonometrically/exponentially-fitted methods are proposed (see, e.g., [26, 27, 28, 29, 30, 31, 32]). Some authors, such as González, et al. [33] and Franco [13], are interested in numerical integrators of Runge-Kutta-Nyström type adapted to initial value problems of the form

$$\begin{cases} y''(t) + \omega^2 y(t) = f\big(y(t)\big),\ t \in [t_0, T], \\ y(t_0) = y_0,\ y'(t_0) = y'_0, \end{cases} \tag{1}$$

where ω is the main frequency and $\omega > 0$. More recently, a new family of extended Runge-Kutta-Nyström (ERKN) methods are proposed by Yang, et al. [18] for one-dimensional perturbed oscillators and systems of these oscillators with ω^2 being a diagonal matrix. Furthermore, with the methodology in [18], a standard form of multidimensional ERKN integrators for the general system (1) is formulated by Wu, et al. [19], where ω^2 is a symmetric positive semi-definite matrix and implicitly contains the frequencies of the problem. The corresponding order conditions are also derived by the authors based on the B-series theory associated with the extended Nyström trees (EN-trees) [19]. These methods preserve the oscillatory feature of the unperturbed oscillators, not only for the updates but also for the internal stages. Numerical results have shown that ERKN methods are superior to other methods for oscillatory systems.

In this paper, we investigate the multi-symplectic ERKN (MSERKN) methods for wave equations as Hamiltonian PDEs. In Section 2, we discuss the conservation laws for Hamiltonian wave equations. In Section 3, we show that the discretization in time and space for Hamiltonian wave equations with two symplectic ERKN (SERKN) methods leads to a multi-symplectic integrator. In Section 4, explicit multi-symplectic schemes are constructed based on the SERKN methods and a symplectic Partitioned Runge-Kutta (SPRK) method. Section 5 is devoted to the numerical experiments, including the dispersive properties of the schemes proposed in this paper. Some conclusions are given in the last section.

2. Conservation laws and multi-symplectic structures of wave equations

2.1. Multi-symplectic conservation laws and multi-symplectic integrators

A multi-Hamiltonian PDE in one time dimension and one space dimension is a PDE that can be formulated in the following way (see [34]). Let M and K be any skew-symmetric real $n \times n$ matrices ($n \geq 3$) and let $S : \mathbb{R}^n \to \mathbb{R}$ be any smooth function of the state variable z. Then a system of the following form is called a Hamiltonian system on a multi-symplectic structure:

$$Mz_t + Kz_x = \nabla_z S(z),\ z \in \mathbb{R}^n,\ (x,t) \in \mathbb{R}^2, \tag{2}$$

where ∇_z is the gradient operator corresponding to the standard inner product on $\mathbb{R}^n$ denoted by $\langle \cdot, \cdot \rangle$.

The Hamiltonian system (2) is multi-symplectic in the sense that it is associated with two-forms:

$$\zeta = \frac{1}{2} dz \wedge Mdz,\ \kappa = \frac{1}{2} dz \wedge Kdz,$$

which define a space-time symplectic structure governed by the multi-symplectic conservation law

$$\partial_t \zeta + \partial_x \kappa = 0. \tag{3}$$

Let L be the length of the spatial domain. Then integrating (3) over the spatial domain leads to

$$\frac{d}{dt} \int_{-L/2}^{L/2} \zeta dx + \kappa|_{x=L/2} - \kappa|_{x=-L/2} = 0.$$

This equation, under appropriate boundary conditions such as $z(L/2,t) = z(-L/2,t)$, results in the conservation of global symplecticity: $\frac{d}{dt}\overline{\zeta}(z) = 0$, where

$$\overline{\zeta}(z) = \int_{-L/2}^{L/2} \zeta(z)dx. \tag{4}$$

$\overline{\zeta}(z)$ is a reminder indicating that the two-form ζ is integrated over all space. A properly chosen semi-discretization of this system may lead to a system of Hamiltonian ODEs with a symplectic form given by a discrete version of (4). An overview of this viewpoint in terms of symplectic time-integration methods is given by McLachlan [35].

Two other conservation laws for the energy and the momentum respectively follow from (3). The local energy conservation law is

$$\partial_t E(z) + \partial_x F(z) = 0, \tag{5}$$

where $E(z) = S(z) - \frac{1}{2}z^T K z_x$ is the energy density and $F(z) = \frac{1}{2}z^T K z_t$ is the energy flux. The local momentum conservation law is

$$\partial_t I(z) + \partial_x G(z) = 0, \tag{6}$$

where $I(z) = \frac{1}{2}z^T M z_x$ and $G(z) = S(z) - \frac{1}{2}z^T M z_t$ are the momentum density and the momentum flux, respectively. Similar to the conservation of multi-symplecticity, integrating the local conservation laws (5) and (6) over the spatial domain in $\mathbb{R}^n$ with periodic boundary conditions leads to global conservation laws

$$\frac{d}{dt}\varepsilon(z) = 0 \text{ and } \frac{d}{dt}\mathcal{I}(z) = 0, \tag{7}$$

where $\varepsilon(z) = \int_{-L/2}^{L/2} E(z)dx$ and $\mathcal{I}(z) = \int_{-L/2}^{L/2} I(z)dx$. We note that the global conservation of energy or momentum (7) is necessary but not sufficient for the local conservation of energy or momentum.

When it comes to the numerical integration, the symplecticity of numerical integrators should be determined.

Definition 2.1. *[34] A numerical scheme is called multi-symplectic if it preserves a discrete conservation law of* (3).

An alternative definition of multi-symplectic integrators based on a discrete form of the symplectic conservation law is suggested by Bridges and Reich [3]. It has been shown that popular methods such as the centered Preissman scheme and the leap-frog method are multi-symplectic and that such schemes have remarkable properties of conserving local energy and momentum.

2.2. Conservation laws for wave equations

Consider the following nonlinear wave equation (see [36]):

$$u_{tt} - u_{xx} + V'(u) = 0, \tag{8}$$

where $V(u)$ is certain smooth function and u is a scalar function. Introducing two new variables $v = u_t$ and $w = u_x$, we can write (8) as

$$\begin{cases} v_t - w_x + V'(u) = 0, \\ v = u_t, \\ w = u_x. \end{cases}$$

By taking $z = (u, v, w)^T \in \mathbb{R}^3$, we can obtain a first order PDE system of the abstract form (2) corresponding to (8) (see, e.g., [11]), with

$$M = \begin{pmatrix} 0 & -1 & 0 \\ 1 & 0 & 0 \\ 0 & 0 & 0 \end{pmatrix}, \; K = \begin{pmatrix} 0 & 0 & 1 \\ 0 & 0 & 0 \\ -1 & 0 & 0 \end{pmatrix},$$

and the Hamiltonian is $S(z) = \dfrac{1}{2}(v^2 - w^2) + V(u)$. As mentioned in Subsection 2.1, this system has the multi-symplectic conservation law (3), where ζ and κ are the pre-symplectic forms

$$\zeta = \frac{1}{2}dz \wedge Mdz = dv \wedge du, \tag{9}$$

$$\kappa = \frac{1}{2}dz \wedge Kdz = du \wedge dw. \tag{10}$$

By applying the general approach of deriving the local energy and momentum conservation law to the nonlinear wave equation (8), as discussed in the previous subsection, it follows that the local energy conservation law is (5) with $E(z) = \dfrac{1}{2}(v^2 + w^2) + V(u)$ and $F(z) = -vw$. Meanwhile, the local momentum conservation law is (6) with $I(z) = vw$ and $G(z) = -\dfrac{1}{2}(v^2 + w^2) + V(u)$ (see [11]).

3. Extended RKN discretization of wave equations

3.1. Extended RKN methods for ODEs

In [18], Yang, et al. investigate ERKN methods for the IVP (1) of the following form :

$$\begin{cases} Y_i = \phi_0(c_i\nu)y_n + c_i\phi_1(c_i\nu)hy'_n + h^2\sum\limits_{j=1}^{s}\bar{a}_{ij}(\nu)f(t_n + c_jh, Y_j), \quad i = 1, \dots, s, \\ y_{n+1} = \phi_0(\nu)y_n + \phi_1(\nu)hy'_n + h^2\sum\limits_{i=1}^{s}\bar{b}_i(\nu)f(t_n + c_ih, Y_i), \\ y'_{n+1} = -\nu w\phi_1(\nu)y_n + \phi_0(\nu)y'_n + h\sum\limits_{i=1}^{s}b_i(\nu)f(t_n + c_ih, Y_i), \end{cases} \tag{11}$$

where $\bar{a}_{ij}(\nu), b_i(\nu)$ and $\bar{b}_i(\nu)$, $i, j = 1, \dots, s$, are assumed to be even functions of $\nu = h\omega$, $\phi_0(\nu) = \cos(\nu)$, and $\phi_1(\nu) = \dfrac{\sin(\nu)}{\nu}$. We denote (11) by $\{c_i, b_i, \bar{b}_i, \bar{a}_{ij}, \omega\}$ in this paper.

Very recently, ERKN methods are considered for Hamiltonian ODEs, whose solutions exhibit a periodic or oscillatory character. The coefficients of these methods depend on the product of the step size h and the fitted frequency ω, and the methods can be expressed in Butcher tableau as :

$$\begin{array}{c|c} c & \bar{A}(\nu) \\ \hline & \bar{b}^T(\nu) \\ \hline & b^T(\nu) \end{array} \quad = \quad \begin{array}{c|ccc} c_1 & \bar{a}_{11}(\nu) & \dots & \bar{a}_{1s}(\nu) \\ \vdots & \vdots & \ddots & \vdots \\ c_s & \bar{a}_{s1}(\nu) & \cdots & \bar{a}_{ss}(\nu) \\ \hline & \bar{b}_1(\nu) & \cdots & \bar{b}_s(\nu) \\ \hline & b_1(\nu) & \cdots & b_s(\nu) \end{array}$$

The symplecticity conditions for ERKN methods are given by the next theorem.

Theorem 3.1. *(Wu, et al. [37, 20]) If the coefficients of an s-stage ERKN method satisfy the following conditions*

$$\begin{cases} \bar{b}_i(\nu)\left(\phi_0(\nu) + \dfrac{c_i\nu^2\phi_1(\nu)\phi_1(c_i\nu)}{\phi_0(c_i\nu)}\right) = b_i(\nu)\left(\phi_1(\nu) - \dfrac{c_i\phi_0(\nu)\phi_1(c_i\nu)}{\phi_0(c_i\nu)}\right), \\ \quad i = 1, \dots, s, \\ b_i(\nu)\left(\bar{b}_j(\nu) - \dfrac{\bar{a}_{ij}(\nu)\phi_0(\nu)}{\phi_0(c_i\nu)}\right) - \bar{b}_i(\nu)\bar{a}_{ij}(\nu)\dfrac{\nu^2\phi_1(\nu)}{\phi_0(c_i\nu)} \\ \quad = b_j(\nu)\left(\bar{b}_i(\nu) - \dfrac{\bar{a}_{ji}(\nu)\phi_0(\nu)}{\phi_0(c_j\nu)}\right) - \bar{b}_j(\nu)\bar{a}_{ji}(\nu)\dfrac{\nu^2\phi_1(\nu)}{\phi_0(c_j\nu)}, \quad i, j = 1, \dots, s, \end{cases} \tag{12}$$

then the method is symplectic.

Remark 3.1. When $\omega \to 0$, the scheme (11) reduces to a classical RKN method in Hairer, et al. [38]. In this case, the symplecticity conditions of (12) become

$$\begin{cases} \bar{b}_i = (1-c_i)b_i, & i = 1,\dots,s, \\ b_i(\bar{b}_j - \bar{a}_{ij}) = b_j(\bar{b}_i - \bar{a}_{ji}), & i \le j = 1,\dots,s, \end{cases}$$

which are obtained by Suris [39] for the symplecticity of an s-stage RKN method.

3.2. Multi-symplectic extended RKN discretization

In order to derive the new MSERKN methods, we first consider the discretization of the equation (8) by employing the following two different SERKN methods in temporal and spatial directions, respectively:

$$\begin{array}{c|ccc} c_1 & \bar{a}_{11}(\nu_t) & \dots & \bar{a}_{1r}(\nu_t) \\ \vdots & \vdots & \ddots & \vdots \\ c_r & \bar{a}_{r1}(\nu_t) & \cdots & \bar{a}_{rr}(\nu_t) \\ \hline & \bar{b}_1(\nu_t) & \cdots & \bar{b}_r(\nu_t) \\ \hline & b_1(\nu_t) & \cdots & b_r(\nu_t) \end{array} \qquad \begin{array}{c|ccc} \tilde{c}_1 & \hat{a}_{11}(\nu_x) & \dots & \hat{a}_{1s}(\nu_x) \\ \vdots & \vdots & \ddots & \vdots \\ \tilde{c}_s & \hat{a}_{s1}(\nu_x) & \cdots & \hat{a}_{ss}(\nu_x) \\ \hline & \hat{b}_1(\nu_x) & \cdots & \hat{b}_s(\nu_x) \\ \hline & \tilde{b}_1(\nu_x) & \cdots & \tilde{b}_s(\nu_x) \end{array}$$

Theorem 3.2. *Assume that a method results from the temporal discretization of the wave equation* (8) *with an r-stage SERKN scheme $\{c_i, b_i, \bar{b}_i, \bar{a}_{ij}, \omega_t\}$ and spatial discretization with an s-stage SERKN scheme $\{\tilde{c}_i, \tilde{b}_i, \hat{b}_i, \hat{a}_{ij}, \omega_x\}$, where the coefficients satisfy the symplectic conditions*

$$\begin{cases} \bar{b}_i(\nu_t)\left(\phi_0(\nu_t) + \dfrac{c_i{\nu_t}^2\phi_1(\nu_t)\phi_1(c_i\nu_t)}{\phi_0(c_i\nu_t)}\right) = b_i(\nu_t)\left(\phi_1(\nu_t) - \dfrac{c_i\phi_0(\nu_t)\phi_1(c_i\nu_t)}{\phi_0(c_i\nu_t)}\right), \\ \qquad i = 1,\dots,r, \\ b_i(\nu_t)\left(\bar{b}_j(\nu_t) - \dfrac{\bar{a}_{ij}(\nu_t)\phi_0(\nu_t)}{\phi_0(c_i\nu_t)}\right) - \bar{b}_i(\nu_t)\bar{a}_{ij}(\nu_t)\dfrac{{\nu_t}^2\phi_1(\nu_t)}{\phi_0(c_i\nu_t)} \\ \qquad = b_j(\nu_t)\left(\bar{b}_i(\nu_t) - \dfrac{\bar{a}_{ji}(\nu_t)\phi_0(\nu_t)}{\phi_0(c_j\nu_t)}\right) - \bar{b}_j(\nu_t)\bar{a}_{ji}(\nu_t)\dfrac{{\nu_t}^2\phi_1(\nu_t)}{\phi_0(c_j\nu_t)}, \\ \qquad i, j = 1,\dots,r, \end{cases} \tag{13}$$

and

$$\begin{cases} \hat{b}_i(\nu_x)\left(\phi_0(\nu_x) + \dfrac{\tilde{c}_i{\nu_x}^2\phi_1(\nu_x)\phi_1(\tilde{c}_i\nu_x)}{\phi_0(\tilde{c}_i\nu_x)}\right) = \tilde{b}_i(\nu_x)\left(\phi_1(\nu_x) - \dfrac{\tilde{c}_i\phi_0(\nu_x)\phi_1(\tilde{c}_i\nu_x)}{\phi_0(\tilde{c}_i\nu_x)}\right), \\ \qquad i = 1,\dots,s, \\ \tilde{b}_i(\nu_x)\left(\hat{b}_j(\nu_x) - \dfrac{\hat{a}_{ij}(\nu_x)\phi_0(\nu_x)}{\phi_0(\tilde{c}_i\nu_x)}\right) - \hat{b}_i(\nu_x)\hat{a}_{ij}(\nu_x)\dfrac{{\nu_x}^2\phi_1(\nu_x)}{\phi_0(\tilde{c}_i\nu_x)} \\ \qquad = \tilde{b}_j(\nu_x)\left(\hat{b}_i(\nu_x) - \dfrac{\hat{a}_{ji}(\nu_x)\phi_0(\nu_x)}{\phi_0(\tilde{c}_j\nu_x)}\right) - \hat{b}_j(\nu_x)\hat{a}_{ji}(\nu_x)\dfrac{{\nu_x}^2\phi_1(\nu_x)}{\phi_0(\tilde{c}_j\nu_x)}, \\ \qquad i, j = 1,\dots,s, \end{cases} \tag{14}$$

respectively. The method is said to be multi-symplectic in the sense that it satisfies the discrete multi-symplectic conservation law

$$\begin{aligned} &\sum_{i=1}^{s}\left(\frac{1}{\phi_0(\tilde{c}_i\nu_x)}\left(\tilde{b}_i\phi_0(\nu_x) + \hat{b}_i\nu_x^2\phi_1(\nu_x)\right)\right)(dv_{m,i}^{n+1} \wedge du_{m,i}^{n+1} - dv_{m,i}^{n} \wedge du_{m,i}^{n})h \\ + \;&\sum_{k=1}^{r}\left(\frac{1}{\phi_0(c_k\nu_t)}\left(b_k\phi_0(\nu_t) + \bar{b}_k\nu_t^2\phi_1(\nu_t)\right)\right)(du_{m+1}^{n,k} \wedge dw_{m+1}^{n,k} - du_{m}^{n,k} \wedge dw_{m}^{n,k})\tau = 0, \end{aligned} \tag{15}$$

where τ and h are the step-size of time and space, respectively.

Proof. We first apply an s-stage SERKN method with the spatial discretization and rewrite equation (8) as

$$\begin{cases} U_i = \phi_0(\tilde{c}_i\nu_x)u_m + \tilde{c}_i\phi_1(\tilde{c}_i\nu_x)hw_m + h^2\sum_{j=1}^{s}\hat{a}_{ij}(\nu_x)f_j, \qquad i=1,\ldots,s, \\ u_{m+1} = \phi_0(\nu_x)u_m + \phi_1(\nu_x)hw_m + h^2\sum_{i=1}^{s}\hat{b}_i(\nu_x)f_i, \\ w_{m+1} = -\nu_x\omega_x\phi_1(\nu_x)u_m + \phi_0(\nu_x)w_m + h\sum_{i=1}^{s}\tilde{b}_i(\nu_x)f_i, \end{cases}$$

where $f_i = f(U_i) = \omega_x^2U_i + \partial_{xx}U_i$. Having $\phi_0(\nu) = \cos(\nu)$ and $\phi_1(\nu) = \dfrac{\sin(\nu)}{\nu}$ in mind, we proceed with

$$\begin{aligned} du_{m+1}\wedge dw_{m+1} = \;& du_m\wedge dw_m + h\sum_{i=1}^{s}\big(\tilde{b}_i(\nu_x)\phi_0(\nu_x) + \hat{b}_i(\nu_x)\nu_x^2\phi_1(\nu_x)\big)du_m\wedge df_i \\ & + h^2\sum_{i=1}^{s}\big(\tilde{b}_i(\nu_x)\phi_1(\nu_x) - \hat{b}_i(\nu_x)\phi_0(\nu_x)\big)dw_m\wedge df_i + h^3\sum_{i,j=1}^{s}\hat{b}_i(\nu_x)\tilde{b}_j(\nu_x)df_i\wedge df_j \\ = \;& du_m\wedge dw_m + h\sum_{i=1}^{s}\left(\frac{1}{\phi_0(\tilde{c}_i\nu_x)}\big(\tilde{b}_i(\nu_x)\phi_0(\nu_x) + \hat{b}_i(\nu_x)\nu_x^2\phi_1(\nu_x)\big)\right)dU_i\wedge df_i \\ & - h^2\sum_{i=1}^{s}\left(\big(\tilde{b}_i(\nu_x)\phi_0(\nu_x)+\hat{b}_i(\nu_x)\nu_x^2\phi_1(\nu_x)\big)\frac{\tilde{c}_i\phi_1(\tilde{c}_i\nu_x)}{\phi_0(\tilde{c}_i\nu_x)} - \tilde{b}_i(\nu_x)\phi_1(\nu_x)+\hat{b}_i(\nu_x)\phi_0(\nu_x)\right)dw_m\wedge df_i \\ & + h^3\sum_{i,j=1}^{s}\left(\frac{\tilde{b}_i(\nu_x)\phi_0(\nu_x) + \hat{b}_i(\nu_x)\nu_x^2\phi_1(\nu_x)}{\phi_0(\tilde{c}_i\nu_x)}\hat{a}_{ij} + \hat{b}_i(\nu_x)\tilde{b}_j(\nu_x)\right)df_i\wedge df_j. \end{aligned}$$

Together with (14), this is further transformed to

$$\begin{aligned} du_{m+1}\wedge dw_{m+1} = \;& du_m\wedge dw_m + h\sum_{i=1}^{s}\left(\frac{1}{\phi_0(\tilde{c}_i\nu_x)}\big(\tilde{b}_i(\nu_x)\phi_0(\nu_x) + \hat{b}_i(\nu_x)\nu_x^2\phi_1(\nu_x)\big)\right)dU_i\wedge df_i \\ = \;& du_m\wedge dw_m + h\sum_{i=1}^{s}\left(\frac{1}{\phi_0(\tilde{c}_i\nu_x)}\big(\tilde{b}_i(\nu_x)\phi_0(\nu_x) + \hat{b}_i(\nu_x)\nu_x^2\phi_1(\nu_x)\big)\right)dU_i\wedge(\omega_x^2dU_i + \partial_{xx}dU_i). \end{aligned}$$

Then, we obtain the following semi-symplectic conservation law in space:

$$du_{m+1}\wedge dw_{m+1} = du_m\wedge dw_m + h\sum_{i=1}^{s}\left(\frac{1}{\phi_0(\tilde{c}_i\nu_x)}\big(\tilde{b}_i(\nu_x)\phi_0(\nu_x) + \hat{b}_i(\nu_x)\nu_x^2\phi_1(\nu_x)\big)\right)dU_i\wedge\partial_x dW_i. \tag{16}$$

The next step is the discretization in time over a time interval $[0,\tau]$. For simplicity, we set $m = 0$ and assume that $x_m = 0$. We use the r-stage SERKN method and obtain

$$\begin{cases} U_i^k = \phi_0(c_k\nu_t)u_i^0 + c_k\phi_1(c_k\nu_t)\tau v_i^0 + \tau^2\sum_{l=1}^{r}\bar{a}_{kl}(\nu_t)g_i^l, \qquad k=1,\ldots,r, \\ u_i^1 = \phi_0(\nu_t)u_i^0 + \phi_1(\nu_t)\tau v_i^0 + \tau^2\sum_{k=1}^{r}\bar{b}_k(\nu_t)g_i^k, \\ v_i^1 = -\nu_t\omega_t\phi_1(\nu_t)u_i^0 + \phi_0(\nu_t)v_i^0 + \tau\sum_{k=1}^{r}b_k(\nu_t)g_i^k. \end{cases}$$

Here, we introduce the notation

$$\begin{aligned} & U_i^k \approx u(\tilde{c}_ih,\ c_k\tau),\ V_i^k \approx v(\tilde{c}_ih,\ c_k\tau),\ u_i^1 \approx u(\tilde{c}_ih,\tau),\ v_i^1 \approx v(\tilde{c}_ih,\tau), \\ & g_i^k = g(U_i^k) = \omega_t^2U_i^k + \partial_{tt}U_i^k. \end{aligned}$$

Likewise, we can obtain the identity

$$du_i^1\wedge dv_i^1 = du_i^0\wedge v_i^0 + \tau\sum_{k=1}^{r}\left(\frac{1}{\phi_0(c_k\nu_t)}\big(b_k(\nu_t)\phi_0(\nu_t) + \bar{b}_k(\nu_t)\nu_t^2\phi_1(\nu_t)\big)\right)dU_i^k\wedge\partial_t dV_i^k.$$

This is the symplectic conservation law in time direction. For any $x = x_{m,i} = x_m + \tilde{c}_i h, t = t_{n,k} = t_n + c_k \tau$, the above identity can be transformed to

$$du_{m,i}^{n+1} \wedge dv_{m,i}^{n+1} - du_{m,i}^{n} \wedge dv_{m,i}^{n} = \tau \sum_{k=1}^{r} \left(\frac{1}{\phi_0(c_k \nu_t)} \big(b_k(\nu_t)\phi_0(\nu_t) + \bar{b}_k(\nu_t)\nu_t^2 \phi_1(\nu_t) \big) \right) (dU_{m,i}^{n,k} \wedge \partial_t dV_{m,i}^{n,k}). \quad (17)$$

Next, we rewrite (16) for $t = t_{n,k}$ as

$$du_{m+1}^{n,k} \wedge dw_{m+1}^{n,k} - du_{m}^{n,k} \wedge w_{m}^{n,k} = h \sum_{i=1}^{s} \left(\frac{1}{\phi_0(\tilde{c}_i \nu_x)} \big(\tilde{b}_i(\nu_x)\phi_0(\nu_x) + \hat{b}_i(\nu_x)\nu_x^2 \phi_1(\nu_x) \big) \right) (dU_{m,i}^{n,k} \wedge \partial_x dW_{m,i}^{n,k}). \quad (18)$$

It finally follows from (17) and (18) that the discrete multi-symplectic conservation law (15) holds. □

Meanwhile, the fully-discrete scheme for (8) is given by

$$\begin{cases} U_{m,i}^{n,k} = \phi_0(\tilde{c}_i\nu_x)u_m^{n,k} + \tilde{c}_i\phi_1(\tilde{c}_i\nu_x)hw_m^{n,k} + h^2 \sum\limits_{j=1}^{s} \hat{a}_{ij}(\nu_x) f_{m,j}^{n,k}, \qquad i = 1,\dots,s, \\ u_{m+1}^{n,k} = \phi_0(\nu_x)u_m^{n,k} + \phi_1(\nu_x)hw_m^{n,k} + h^2 \sum\limits_{i=1}^{s} \hat{b}_i(\nu_x) f_{m,i}^{n,k}, \\ w_{m+1}^{n,k} = -\nu_x\omega_x\phi_1(\nu_x)u_m^{n,k} + \phi_0(\nu_x)w_m^{n,k} + h \sum\limits_{i=1}^{s} \tilde{b}_i(\nu_x) f_{m,i}^{n,k}, \\ U_{m,i}^{n,k} = \phi_0(c_k\nu_t)u_{m,i}^{n} + c_k\phi_1(c_k\nu_t)\tau v_{m,i}^{n} + \tau^2 \sum\limits_{l=1}^{r} \bar{a}_{kl}(\nu_t) g_{m,i}^{n,l}, \qquad k = 1,\dots,r, \\ u_{m,i}^{n+1} = \phi_0(\nu_t)u_{m,i}^{n} + \phi_1(\nu_t)\tau v_{m,i}^{n} + \tau^2 \sum\limits_{k=1}^{r} \bar{b}_k(\nu_t) g_{m,i}^{n,k}, \\ v_{m,i}^{n+1} = -\nu_t\omega_t\phi_1(\nu_t)u_{m,i}^{n} + \phi_0(\nu_t)v_{m,i}^{n} + \tau \sum\limits_{k=1}^{r} b_k(\nu_t) g_{m,i}^{n,k}, \end{cases} \quad (19)$$

where we have used the following notation:

$$\begin{aligned} &U_{m,i}^{n,k} \approx u(x_m + \tilde{c}_i h,\ t_n + c_k\tau), \\ &u_{m,i}^{n+1} \approx u(x_m + \tilde{c}_i h, t_n + \tau), \qquad v_{m,i}^{n+1} \approx v(x_m + \tilde{c}_i h, t_n + \tau), \\ &u_{m+1}^{n,k} \approx u(x_m + h, t_n + c_k\tau), \qquad w_{m+1}^{n,k} \approx w(x_m + h, t_n + c_k\tau), \\ &g_{m,i}^{n,k} = g(U_{m,i}^{n,k}) = \omega_t^2 U_{m,i}^{n,k} + \partial_{tt}U_{m,i}^{n,k} = \omega_t^2 U_{m,i}^{n,k} + \partial_{xx}U_{m,i}^{n,k} - V'(U_{m,i}^{n,k}), \\ &f_{m,i}^{n,k} = f(U_{m,i}^{n,k}) = \omega_x^2 U_{m,i}^{n,k} + \partial_{xx}U_{m,i}^{n,k}. \end{aligned}$$

The formula (15) can be understood as the approximation of the integral of (3) over the domain $[x_m, x_{m+1}] \times [t_n, t_{n+1}]$. That is, (15) approximates

$$\begin{aligned} &\int_{x_m}^{x_{m+1}} \big(dv(x, t_{n+1}) \wedge du(x, t_{n+1}) - dv(x, t_n) \wedge du(x, t_n) \big) dx \\ &+ \int_{t_n}^{t_{n+1}} \big(du(x_{m+1}, t) \wedge dw(x_{m+1}, t) - du(x_m, t) \wedge dw(x_m, t) \big) dt = 0, \end{aligned} \quad (20)$$

with SERKN methods for the evaluation of the two integrals.

When the problems with periodic boundary conditions are considered, (15) has another interesting consequence. Let us take the sum of the identity (15) over all spatial grid points $m = 1, \dots, M$ as:

$$\begin{aligned} &\sum_{m=1}^{M} \Bigg\{ \sum_{i=1}^{s} \left(\frac{1}{\phi_0(\tilde{c}_i\nu_x)} \big(\tilde{b}_i(\nu_x)\phi_0(\nu_x) + \hat{b}_i(\nu_x)\nu_x^2\phi_1(\nu_x) \big) \right) (dv_{m,i}^{n+1} \wedge du_{m,i}^{n+1} - dv_{m,i}^{n} \wedge du_{m,i}^{n})h \\ &+ \sum_{k=1}^{r} \left(\frac{1}{\phi_0(c_k\nu_t)} \big(b_k(\nu_t)\phi_0(\nu_t) + \bar{b}_k(\nu_t)\nu_t^2\phi_1(\nu_t) \big) \right) (du_{m+1}^{n,k} \wedge dw_{m+1}^{n,k} - du_{m}^{n,k} \wedge dw_{m}^{n,k})\tau \Bigg\} = 0. \end{aligned} \quad (21)$$

Periodic boundary conditions in space imply

$$
\begin{aligned}
&\sum_{m=1}^{M}\sum_{k=1}^{r}\left(\frac{1}{\phi_0(c_k\nu_t)}\big(b_k(\nu_t)\phi_0(\nu_t)+\bar{b}_k(\nu_t)\nu_t^2\phi_1(\nu_t)\big)\right)(du_{m+1}^{n,k}\wedge dw_{m+1}^{n,k}-du_m^{n,k}\wedge dw_m^{n,k})\tau\\
=&\sum_{k=1}^{r}\left(\frac{1}{\phi_0(c_k\nu_t)}\big(b_k(\nu_t)\phi_0(\nu_t)+\bar{b}_k(\nu_t)\nu_t^2\phi_1(\nu_t)\big)\right)(du_{M+1}^{n,k}\wedge dw_{M+1}^{n,k}-du_1^{n,k}\wedge dw_1^{n,k})\tau=0,
\end{aligned}
$$

which in turn transforms (21) to

$$
\begin{aligned}
&\sum_{m=1}^{M}\sum_{i=1}^{s}\left(\frac{1}{\phi_0(\tilde{c}_i\nu_x)}\big(\tilde{b}_i(\nu_x)\phi_0(\nu_x)+\hat{b}_i(\nu_x)\nu_x^2\phi_1(\nu_x)\big)\right)dv_{m,i}^{n+1}\wedge du_{m,i}^{n+1}\\
=&\sum_{m=1}^{M}\sum_{i=1}^{s}\left(\frac{1}{\phi_0(\tilde{c}_i\nu_x)}\big(\tilde{b}_i(\nu_x)\phi_0(\nu_x)+\hat{b}_i(\nu_x)\nu_x^2\phi_1(\nu_x)\big)\right)dv_{m,i}^{n}\wedge du_{m,i}^{n}.
\end{aligned}
$$

This is precisely the conservation of symplecticity in time. It is also the discretization of the total symplectic conservation (4) with (9).

Remark 3.2. By abuse of notation, we denote the fitted temporal frequency and spatial frequency in the two SERKN methods $\{c_i, b_i, \bar{b}_i, \bar{a}_{ij}, \omega_t\}$ and $\{\tilde{c}_i, \tilde{b}_i, \hat{b}_i, \hat{a}_{ij}, \omega_x\}$ by ω_t and ω_x, respectively. Obviously, when $\omega_t \to 0$ and $\omega_x \to 0$, the MSERKN methods become multi-symplectic RKN (MSRKN) methods.

Remark 3.3. Theorem 3.2 shows that concatenation of SERKN methods can produce a multi-symplectic integrator for Hamiltonian wave equations. It is remarked that the above idea may apply equally to some other Hamiltonian PDEs.

For Hamiltonian PDEs with oscillations in both space and time directions, two SERKN methods are used in space and time respectively. For the case that oscillation exists only in time direction, we propose the following multi-symplectic discretizations.

Theorem 3.3. *The wave equation* (8) *discretized by an SPRK method in space and an SERKN method in time has a discrete multi-symplectic conservation law.*

The proof is similar to that of Theorem 3.2. As an example, we use SERKN discretization in time and the following SPRK discretization in space (which can be regarded as the Störmer-Verlet formula):

$$
\underbrace{\begin{array}{c|cc} 0 & 0 & 0\\ 1 & \frac{1}{2} & \frac{1}{2}\\ \hline & \frac{1}{2} & \frac{1}{2}\end{array}}_{u}
\qquad\qquad
\underbrace{\begin{array}{c|cc} \frac{1}{2} & \frac{1}{2} & 0\\ \frac{1}{2} & \frac{1}{2} & 0\\ \hline & \frac{1}{2} & \frac{1}{2}\end{array}}_{w}
\tag{22}
$$

Proof. We first apply the SPRK method (22) to the spatial discretization for u and w respectively and obtain

$$
\begin{cases}
U_{m,1} = u_m,\\
U_{m,2} = u_{m+1},\\
W_{m,1} = w_m + \dfrac{h}{2}\partial_{xx}u_m,\\
W_{m,2} = w_m + \dfrac{h}{2}\partial_{xx}u_m,\\
u_{m+1} = u_m + \dfrac{h}{2}(W_{m,1}+W_{m,2}),\\
w_{m+1} = w_m + \dfrac{h}{2}(\partial_{xx}U_{m,1}+\partial_{xx}U_{m,2}).
\end{cases}
\tag{23}
$$

Then proceed with

$$\begin{aligned} du_{m+1}\wedge dw_{m+1} &= d(u_m+hw_m+\frac{h^2}{2}\partial_{xx}u_m)\wedge d(w_m+\frac{h}{2}\partial_{xx}u_m+\frac{h}{2}\partial_{xx}u_{m+1})\\ &= du_m\wedge dw_m+\frac{h}{2}du_m\wedge\partial_{xx}du_m+\frac{h}{2}du_{m+1}\wedge\partial_{xx}du_{m+1}\\ &= du_m\wedge dw_m+\frac{h}{2}dU_{m,1}\wedge\partial_{xx}dU_{m,1}+\frac{h}{2}dU_{m,2}\wedge\partial_{xx}dU_{m,2}\\ &= du_m\wedge dw_m+\frac{h}{2}dU_{m,1}\wedge\partial_{x}dW_{m,1}+\frac{h}{2}dU_{m,2}\wedge\partial_{x}dW_{m,2}\\ &= du_m\wedge dw_m+\frac{h}{2}\sum_{i=1}^{2}(dU_{m,i}\wedge\partial_x dW_{m,i}). \end{aligned}$$

That is,

$$du_{m+1}\wedge dw_{m+1}-du_m\wedge dw_m=\frac{h}{2}\sum_{i=1}^{2}(dU_{m,i}\wedge\partial_x dW_{m,i}). \tag{24}$$

For $t=t_{n,k}$, we rewrite (24) as

$$du^{n,k}_{m+1}\wedge dw^{n,k}_{m+1}-du^{n,k}_m\wedge dw^{n,k}_m=\frac{h}{2}\sum_{i=1}^{2}(dU^{n,k}_{m,i}\wedge\partial_x dW^{n,k}_{m,i}). \tag{25}$$

It follows from (17) and (25) that the multi-symplectic conservation law is

$$\begin{aligned} &\sum_{i=1}^{2}\frac{1}{2}(dv^{n+1}_{m,i}\wedge du^{n+1}_{m,i}-dv^{n}_{m,i}\wedge du^{n}_{m,i})h\\ +\ &\sum_{k=1}^{r}\left(\frac{1}{\phi_0(c_k\nu_t)}\left(b_k(\nu_t)\phi_0(\nu_t)+\bar{b}_k(\nu_t)\nu_t^2\phi_1(\nu_t)\right)\right)(du^{n,k}_{m+1}\wedge dw^{n,k}_{m+1}-du^{n,k}_m\wedge dw^{n,k}_m)\tau=0. \end{aligned} \tag{26}$$

□

Similarly, we can also obtain the following fully-discrete scheme for (8)

$$\begin{cases} u^{n,k}_{m+1}=u^{n,k}_m+hw^{n,k}_m+\dfrac{h^2}{2}\partial_{xx}u^{n,k}_m,\\ w^{n,k}_{m+1}=w^{n,k}_m+\dfrac{h}{2}(\partial_{xx}u^{n,k}_m+\partial_{xx}u^{n,k}_{m+1}),\\ U^{n,k}_m=\phi_0(c_k\nu_t)u^n_m+c_k\phi_1(c_k\nu_t)\tau v^n_m+\tau^2\sum_{l=1}^{r}\bar{a}_{kl}(\nu_t)g^{n,l}_m, \qquad k=1,\dots,r,\\ u^{n+1}_m=\phi_0(\nu_t)u^n_m+\phi_1(\nu_t)\tau v^n_m+\tau^2\sum_{k=1}^{r}\bar{b}_k(\nu_t)g^{n,k}_m,\\ v^{n+1}_m=-\nu_t\omega_t\phi_1(\nu_t)u^n_m+\phi_0(\nu_t)v^n_m+\tau\sum_{k=1}^{r}b_k(\nu_t)g^{n,k}_m. \end{cases} \tag{27}$$

4. Construction of explicit multi-symplectic schemes

Based on the general framework presented in Section 3, a large number of novel multi-symplectic schemes can be constructed. Here, an undoubted fact is that, symplectic Runge-Kutta schemes for the integration of general Hamiltonian systems are usually implicit, and multi-symplectic integrators constructed by concatenating symplectic Runge-Kutta methods and/or symplectic partitioned Runge-Kutta methods are usually implicit. Thus, in practice, one has to solve implicit algebraic equations, often by using some iterative approximation methods. In this case, the resulting integration scheme may no longer be symplectic. The advantage of explicit symplectic integrators, when compared with fully implicit or partly implicit methods, is that they do not require the solution of large and complicated systems of nonlinear algebraic or transcendental equations. Therefore, it is clear that the computational cost of an implicit multi-symplectic method is usually higher than that of an explicit one. Consequently, in this section, we construct two explicit multi-symplectic schemes, which are actually two multi-symplectic extended leap-frog methods. It can be observed that when $\omega_x\to 0,\omega_t\to 0$, these two new schemes Eleap-frogI and Eleap-frogII reduce to classical leap-frog schemes.

4.1. Extended leap-frog scheme I: An explicit multi-symplectic ERKN scheme

In this subsection, we pay attention to constructing an explicit 2-stage MSERKN scheme of order 2. First of all, since $\partial_{xx}U_{m,i}^{n,k}$ appear in (19), we observe that we cannot obtain $u_{m,i}^{n+1}$ and $v_{m,i}^{n+1}$ explicitly provided that $\partial_{xx}U_{m,i}^{n,k}$ could not be expressed explicitly. This means that, even if we use explicit SERKN methods for both spatial and temporal discretizations, the resulting multi-symplectic scheme may not be necessarily explicit. We take the spatial discretization as an example. If we chose $\tilde{c} = [0,1]^T$, $\hat{b}_1(\nu_x) = \hat{a}_{21}(\nu_x)$, and $\hat{b}_2(\nu_x) = \hat{a}_{22}(\nu_x) = 0$, then $U_{m,1}^{n,k} = u_m^{n,k}$, $U_{m,2}^{n,k} = u_{m+1}^{n,k}$, and the second and third equations in (19) become

$$\begin{cases} u_{m+1}^{n,k} = \phi_0(\nu_x)u_m^{n,k} + \phi_1(\nu_x)hw_m^{n,k} + h^2\hat{b}_1(\nu_x)(\omega_x^2 u_m^{n,k} + \partial_{xx}u_m^{n,k}), \\ w_{m+1}^{n,k} = -\nu_x\omega_x\phi_1(\nu_x)u_m^{n,k} + \phi_0(\nu_x)w_m^{n,k} + h\tilde{b}_1(\nu_x)(\omega_x^2 u_m^{n,k} + \partial_{xx}u_m^{n,k}) \\ \qquad\qquad + h\tilde{b}_2(\nu_x)(\omega_x^2 u_{m+1}^{n,k} + \partial_{xx}u_{m+1}^{n,k}). \end{cases}$$

From this we derive that

$$\partial_{xx}u_m^{n,k} = \frac{u_{m+1}^{n,k} - \phi_0(\nu_x)u_m^{n,k} - \phi_1(\nu_x)hw_m^{n,k}}{h^2\hat{b}_1(\nu_x)} - \omega_x^2 u_m^{n,k},$$

and then

$$\partial_{xx}u_{m+1}^{n,k} = \frac{u_{m+2}^{n,k} - \phi_0(\nu_x)u_{m+1}^{n,k} - \phi_1(\nu_x)hw_{m+1}^{n,k}}{h^2\hat{b}_1(\nu_x)} - \omega_x^2 u_{m+1}^{n,k}.$$

Then it follows that

$$\begin{aligned} w_{m+1}^{n,k} =& -\nu_x\omega_x\phi_1(\nu_x)u_m^{n,k} + \phi_0(\nu_x)w_m^{n,k} + h\tilde{b}_1(\nu_x)(\omega_x^2 u_m^{n,k} + \partial_{xx}u_m^{n,k}) \\ & + h\tilde{b}_2(\nu_x)(\omega_x^2 u_{m+1}^{n,k} + \partial_{xx}u_{m+1}^{n,k}) \\ =& -\nu_x\omega_x\phi_1(\nu_x)u_m^{n,k} + \phi_0(\nu_x)w_m^{n,k} + \frac{\tilde{b}_1(\nu_x)}{h\hat{b}_1(\nu_x)}u_{m+1}^{n,k} - \frac{\tilde{b}_1(\nu_x)}{h\hat{b}_1(\nu_x)}\phi_0(\nu_x)u_m^{n,k} - \frac{\tilde{b}_1(\nu_x)}{\hat{b}_1(\nu_x)}\phi_1(\nu_x)w_m^{n,k} \\ & + \frac{\tilde{b}_2(\nu_x)}{h\hat{b}_1(\nu_x)}u_{m+2}^{n,k} - \frac{\tilde{b}_2(\nu_x)}{h\hat{b}_1(\nu_x)}\phi_0(\nu_x)u_{m+1}^{n,k} - \frac{\tilde{b}_2(\nu_x)}{\hat{b}_1(\nu_x)}\phi_1(\nu_x)w_{m+1}^{n,k}. \end{aligned}$$

Assuming

$$\tilde{b}_1(\nu_x) = \frac{\hat{b}_1\phi_0(\nu_x)}{\phi_1(\nu_x)}, \tag{28}$$

then we have $w_{m+1}^{n,k} = \dfrac{\tilde{b}_2(\nu_x)u_{m+2}^{n,k} - \big(\hat{b}_1(\nu_x)\nu_x^2\phi_1(\nu_x) + \tilde{b}_1(\nu_x)\phi_0(\nu_x)\big)u_m^{n,k} + \big(\tilde{b}_1(\nu_x) - \tilde{b}_2(\nu_x)\phi_0(\nu_x)\big)u_{m+1}^{n,k}}{h\hat{b}_1(\nu_x) + h\tilde{b}_2(\nu_x)\phi_1(\nu_x)}$.

Therefore, from (28), together with the symplectic conditions (13), (14) and order conditions of ERKN methods proposed in [18], we can construct several 2-stage SERKN methods of order 2. In this paper, we consider the following 2-stage SERKN methods of order 2 for the two directional discretizations, which can be expressed in Butcher tableaus:

$$\begin{array}{c|cc} 0 & 0 & 0 \\ 1 & \phi_2(\nu_t) & 0 \\ \hline \bar{b}(\nu_t) & \phi_2(\nu_t) & 0 \\ \hline b(\nu_t) & \dfrac{\phi_0(\nu_t)\phi_2(\nu_t)}{\phi_1(\nu_t)} & \phi_1(\nu_t) - \dfrac{\phi_0(\nu_t)\phi_2(\nu_t)}{\phi_1(\nu_t)} \end{array} \tag{29}$$

$$\begin{array}{c|cc} 0 & 0 & 0 \\ 1 & \phi_2(\nu_x) & 0 \\ \hline \hat{b}(\nu_x) & \phi_2(\nu_x) & 0 \\ \hline \tilde{b}(\nu_x) & \dfrac{\phi_0(\nu_x)\phi_2(\nu_x)}{\phi_1(\nu_x)} & \phi_1(\nu_x) - \dfrac{\phi_0(\nu_x)\phi_2(\nu_x)}{\phi_1(\nu_x)} \end{array} \tag{30}$$

where $\phi_2(\nu) = \dfrac{1-\phi_0(\nu)}{\nu^2}$.

Note that as $\omega_t \to 0,\ \omega_x \to 0$, the above two SERKN methods (29) and (30) for time and space discretizations, respectively, reduce to the same classical 2-stage symplectic RKN (SRKN) method of order 2:

$$
\begin{array}{c|cc}
0 & 0 & 0 \\
1 & \frac{1}{2} & 0 \\
\hline
 & \frac{1}{2} & 0 \\
\hline
 & \frac{1}{2} & \frac{1}{2}
\end{array}
$$

This coincides with the leap-frog method

$$
\frac{q_{n+1} - 2q_n + q_{n-1}}{h^2} = f(q_n)
$$

for problem $\dot{p} = f(q),\ \dot{q} = p$. The leap-frog method can be translated from the following 1-stage SRKN method of order 2 by exchanging the roles of p and q:

$$
\begin{array}{c|c}
\frac{1}{2} & 0 \\
\hline
 & \frac{1}{2} \\
\hline
 & 1
\end{array}
\tag{31}
$$

With the discretizations of the SERKN methods (29) and (30), (19) becomes the following scheme

$$
\begin{cases}
U_m^{n,1} = u_m^n, \\
(\partial_{xx}U)_m^{n,1} = \dfrac{U_{m+1}^{n,1} - 2U_m^{n,1} + U_{m-1}^{n,1}}{2h^2\phi_2(\nu_x)}, \\
U_m^{n,2} = \phi_0(\nu_t)u_m^n + \phi_1(\nu_t)\tau v_m^n + \tau^2\phi_2(\nu_t)\left(\omega_t^2 U_m^{n,1} + \partial_{xx}U_m^{n,1} - V'(U_m^{n,1})\right), \\
(\partial_{xx}U)_m^{n,2} = \dfrac{U_{m+1}^{n,2} - 2U_m^{n,2} + U_{m-1}^{n,2}}{2h^2\phi_2(\nu_x)}, \\
u_m^{n+1} = \phi_0(\nu_t)u_m^n + \phi_1(\nu_t)\tau v_m^n + \tau^2\phi_2(\nu_t)\left(\omega_t^2 U_m^{n,1} + \partial_{xx}U_m^{n,1} - V'(U_m^{n,1})\right), \\
v_m^{n+1} = -\nu_t\omega_t\phi_1(\nu_t)u_m^n + \phi_0(\nu_t)v_m^n \\
\qquad + \tau\left(b_1(\nu_t)\left(\omega_t^2 U_m^{n,1} + \partial_{xx}U_m^{n,1} - V'(U_m^{n,1})\right) + b_2(\nu_t)\left(\omega_t^2 U_m^{n,2} + \partial_{xx}U_m^{n,2} - V'(U_m^{n,2})\right)\right).
\end{cases}
\tag{32}
$$

In fact, the scheme (32) gives the discretizations for $(\partial_{xx}u)_m^n$ and $(\partial_{tt}u)_m^n$ by $(\partial_{xx}u)_m^n = \dfrac{u_{m+1}^n - 2u_m^n + u_{m-1}^n}{2h^2\phi_2(\nu_x)}$ and $(\partial_{tt}u)_m^n = \dfrac{u_m^{n+1} - 2u_m^n + u_m^{n-1}}{2\tau^2\phi_2(\nu_t)}$, respectively. This also deduces an extended leap-frog scheme:

$$
\frac{u_m^{n+1} - 2u_m^n + u_m^{n-1}}{2\tau^2\phi_2(\nu_t)} = \frac{u_{m+1}^n - 2u_m^n + u_{m-1}^n}{2h^2\phi_2(\nu_x)} - V'(u_m^n).
\tag{33}
$$

We refer to the scheme (33) as Eleap-frogI and use this scheme to solve a linear wave equation (Problem 1) in the next section. Meanwhile, the discretizations of w and v are given by

$$
w_{m+1}^n = \frac{u_{m+2}^n - u_m^n}{2h\phi_1(\nu_x)}, \quad v_m^{n+1} = \frac{u_m^{n+2} - u_m^n}{2\tau\phi_1(\nu_t)}.
$$

Furthermore, we have the following theorem.

Theorem 4.1. *By simply exchanging the roles of u and w in space and u and v in time, the MSERKN scheme given by the following* 1*-stage SERKN methods of order* 2 *for the two directional discretizations can be transformed into the MSERKN scheme* (33)*:*

$$\begin{array}{c|c} \frac{1}{2} & 0 \\ \hline \bar{b}(\nu_t) & \phi_1^2(\frac{\nu_t}{2})\big/2\phi_0(\frac{\nu_t}{2}) \\ \hline b(\nu_t) & \phi_1(\frac{\nu_t}{2}) \end{array} \tag{34}$$

$$\begin{array}{c|c} \frac{1}{2} & 0 \\ \hline \hat{b}(\nu_x) & \phi_1^2(\frac{\nu_x}{2})\big/2\phi_0(\frac{\nu_x}{2}) \\ \hline \tilde{b}(\nu_x) & \phi_1(\frac{\nu_x}{2}) \end{array} \tag{35}$$

Proof. Firstly, the symplecticity of the schemes (34) and (35) can be directly obtained from Theorem 3.1.

Then, we only show the details for the space discretization, and those for the time discretization are similar. Applying the 1-stage SERKN method (35) with the spatial discretization yields

$$\begin{cases} U_1 = \phi_0(\dfrac{\nu_x}{2})u_m + \dfrac{1}{2}\phi_1(\dfrac{\nu_x}{2})hw_m, \\ u_{m+1} = \phi_0(\nu_x)u_m + \phi_1(\nu_x)hw_m + h^2\hat{b}(\nu_x)f_1, \\ w_{m+1} = -\nu_x\omega_x\phi_1(\nu_x)u_m + \phi_0(\nu_x)w_m + h\tilde{b}(\nu_x)f_1, \end{cases} \tag{36}$$

where $f_1 = f(U_1) = \omega_x^2 U_1 + \partial_{xx}U_1$. From the last two equations in (36), we get

$$\begin{aligned} u_{m+1} =& \phi_0(\nu_x)u_m + \phi_1(\nu_x)hw_m + h^2\hat{b}(\nu_x)f_1 \\ =& \phi_0(\nu_x)u_m + \phi_1(\nu_x)hw_m + h^2\hat{b}(\nu_x)\frac{w_{m+1} + \nu_x\omega_x\phi_1(\nu_x)u_m - \phi_0(\nu_x)w_m}{h\tilde{b}(\nu_x)} \\ =& \phi_0(\nu_x)u_m + \phi_1(\nu_x)hw_m + h\frac{\hat{b}(\nu_x)}{\tilde{b}(\nu_x)}w_{m+1} + \nu_x^2\frac{\hat{b}(\nu_x)}{\tilde{b}(\nu_x)}\phi_1(\nu_x)u_m - h\frac{\hat{b}(\nu_x)}{\tilde{b}(\nu_x)}\phi_0(\nu_x)w_m \\ =& u_m + h\frac{\phi_1(\nu_x)}{1+\phi_0(\nu_x)}(w_m + w_{m+1}). \end{aligned}$$

This shows

$$u_{m+1} - u_m = h\frac{\phi_1(\nu_x)}{1+\phi_0(\nu_x)}(w_m + w_{m+1}). \tag{37}$$

The first and last equations of (36) imply

$$\begin{aligned} w_{m+1} =& -\nu_x\omega_x\phi_1(\nu_x)u_m + \phi_0(\nu_x)w_m + h\tilde{b}(\nu_x)f(U_1) \\ =& -\nu_x\omega_x\phi_1(\nu_x)u_m + \phi_0(\nu_x)w_m + h\tilde{b}(\nu_x)(\omega_x^2U_1 + \partial_{xx}U_1) \\ =& -\nu_x\omega_x\phi_1(\nu_x)u_m + \phi_0(\nu_x)w_m + h\tilde{b}(\nu_x)\left(\omega_x^2\phi_0(\frac{\nu_x}{2})u_m + \omega_x^2\frac{1}{2}\phi_1(\frac{\nu_x}{2})hw_m + \partial_{xx}U_1\right) \\ =& w_m + h\phi_1(\frac{\nu_x}{2})\partial_{xx}U_1. \end{aligned} \tag{38}$$

Following the approach to obtaining the leap-frog method by exchanging the roles of p and q in the SRKN method (31), we also exchange the roles of u and w. Then it can be deduced from the first equation of (36), (37) and (38) that

$$\begin{cases} W_1 = \phi_0(\dfrac{\nu_x}{2})w_m + \dfrac{1}{2}\phi_1(\dfrac{\nu_x}{2})h\partial_{xx}u_m, \\ w_{m+1} = w_m + h\dfrac{\phi_1(\nu_x)}{1+\phi_0(\nu_x)}(\partial_{xx}u_m + \partial_{xx}u_{m+1}), \\ u_{m+1} = u_m + h\phi_1(\dfrac{\nu_x}{2})W_1. \end{cases} \tag{39}$$

The first equation of (39) implies

$$w_{m+1/2} = \phi_0(\frac{\nu_x}{2})w_m + \frac{1}{2}\phi_1(\frac{\nu_x}{2})h\partial_{xx}u_m = \phi_0(\frac{\nu_x}{2})\left(w_m + h\frac{\phi_1(\nu_x)}{1+\phi_0(\nu_x)}\partial_{xx}u_m\right), \tag{40}$$

and then

$$w_m = \frac{1}{\phi_0(\frac{\nu_x}{2})}w_{m+1/2} - h\frac{\phi_1(\nu_x)}{1+\phi_0(\nu_x)}\partial_{xx}u_m. \tag{41}$$

Inserting (41) into the second equation of (39) gives

$$w_{m+1} = \frac{1}{\phi_0(\frac{\nu_x}{2})}w_{m+1/2} + h\frac{\phi_1(\nu_x)}{1+\phi_0(\nu_x)}\partial_{xx}u_{m+1},$$

and furthermore,

$$w_m = \frac{1}{\phi_0(\frac{\nu_x}{2})}w_{m-1/2} + h\frac{\phi_1(\nu_x)}{1+\phi_0(\nu_x)}\partial_{xx}u_m.$$

That is,

$$w_{m-1/2} = \phi_0(\frac{\nu_x}{2})\left(w_m - h\frac{\phi_1(\nu_x)}{1+\phi_0(\nu_x)}\partial_{xx}u_m\right) = \phi_0(\frac{\nu_x}{2})w_m - \frac{1}{2}\phi_1(\frac{\nu_x}{2})h\partial_{xx}u_m. \tag{42}$$

Therefore, it follows from (40) and (42) that

$$\begin{cases} w_{m+1/2} + w_{m-1/2} = 2\phi_0(\frac{\nu_x}{2})w_m, \\ w_{m+1/2} - w_{m-1/2} = \phi_1(\frac{\nu_x}{2})h\partial_{xx}u_m. \end{cases} \tag{43}$$

On the other hand, the last equation of (39) means $w_{m+1/2} = \dfrac{u_{m+1} - u_m}{h\phi_1(\frac{\nu_x}{2})}$, which leads to

$$\begin{cases} w_{m+1/2} + w_{m-1/2} = \dfrac{u_{m+1} - u_m + (u_m - u_{m-1})}{h\phi_1(\frac{\nu_x}{2})} = 2\phi_0(\dfrac{\nu_x}{2})w_m, \\ w_{m+1/2} - w_{m-1/2} = \dfrac{u_{m+1} - u_m - (u_m - u_{m-1})}{h\phi_1(\frac{\nu_x}{2})} = \phi_1(\dfrac{\nu_x}{2})h\partial_{xx}u_m. \end{cases} \tag{44}$$

It follows from (44) that

$$\begin{cases} w_m = \dfrac{u_{m+1} - u_{m-1}}{2h\phi_1(\nu_x)} \\ (\partial_{xx}u)_m = \dfrac{u_{m+1} - 2u_m + u_{m-1}}{2h^2\phi_2(\nu_x)}. \end{cases}$$

For the time discretization, it also can be proved that $(\partial_{tt}u)^n = \dfrac{u^{n+1} - 2u^n + u^{n-1}}{2\tau^2\phi_2(\nu_t)}$ and $v_m^{n+1} = \dfrac{u_m^{n+2} - u_m^n}{2\tau\phi_1(\nu_t)}$ holds. □

4.2. *Extended leap-frog scheme II: An explicit multi-symplectic ERKN-PRK scheme*

In this subsection, we construct another explicit multi-symplectic scheme based on Theorem 3.3. We apply the SPRK method (22) to the space discretization, which is equivalent to the Störmer-Verlet that gives the second order central difference of $\partial_{xx}U_m^{n,k}$, and apply the explicit 2-stage SERKN method (29) to the time discretization. Then the multi-symplectic scheme (27) becomes

$$\begin{cases} U_m^{n,1} = u_m^n, \\ (\partial_{xx} U)_m^{n,1} = \dfrac{U_{m+1}^{n,1} - 2U_m^{n,1} + U_{m-1}^{n,1}}{h^2}, \\ U_m^{n,2} = \phi_0(\nu_t) u_m^n + \phi_1(\nu_t)\tau v_m^n + \tau^2 \phi_2(\nu_t) \left(\omega_t^2 U_m^{n,1} + \partial_{xx} U_m^{n,1} - V'(U_m^{n,1}) \right), \\ (\partial_{xx} U)_m^{n,2} = \dfrac{U_{m+1}^{n,2} - 2U_m^{n,2} + U_{m-1}^{n,2}}{h^2}, \\ u_m^{n+1} = \phi_0(\nu_t) u_m^n + \phi_1(\nu_t)\tau v_m^n + \tau^2 \phi_2(\nu_t) \left(\omega_t^2 U_m^{n,1} + \partial_{xx} U_m^{n,1} - V'(U_m^{n,1}) \right), \\ v_m^{n+1} = -\nu_t \omega_t \phi_1(\nu_t) u_m^n + \phi_0(\nu_t) v_m^n \\ \qquad + \tau \left(b_1(\nu_t) \left(\omega_t^2 U_m^{n,1} + \partial_{xx} U_m^{n,1} - V'(U_m^{n,1}) \right) + b_2(\nu_t) \left(\omega_t^2 U_m^{n,2} + \partial_{xx} U_m^{n,2} - V'(U_m^{n,2}) \right) \right). \end{cases} \tag{45}$$

Just like the situation of the scheme Eleap-frogI, it can be observed that this scheme is equivalent to the following form

$$\frac{u_m^{n+1} - 2u_m^n + u_m^{n-1}}{2\tau^2 \phi_2(\nu_t)} = \frac{u_{m+1}^n - 2u_m^n + u_{m-1}^n}{h^2} - V'(u_m^n), \tag{46}$$

and the discretizations of w and v are

$$w_{m+1}^n = \frac{u_{m+2}^n - u_m^n}{2h}, \quad v_m^{n+1} = \frac{u_m^{n+2} - u_m^n}{2\tau \phi_1(\nu_t)}.$$

It is also equivalent to the concatenation of the 1-stage SERKN method (34) of order 2 and SPRK method (22) applied to the temporal and spatial discretizations, respectively.

We refer to the above scheme (46) as Eleap-frogII, and in the next section, we use this scheme to solve a nonlinear wave equation (Problem 2).

4.3. Analysis of linear stability

In this subsection, we pay attention to another significant aspect for those schemes proposed in this paper, namely, the stability. It is known that the attractiveness of explicit schemes relies on the computational efficiency, but such efficiency is always at the cost of stability. Although an application of the linear stability analysis to nonlinear equations cannot be justified, it is found to be effective in numerical experiments. Using the well-known Fourier method [40], we give some linear stability analysis for the explicit multi-symplectic Eleap-frogI scheme, and the stability for scheme Eleap-frogII can be analyzed in the similar way.

Set

$$u_m^n = \hat{u}^n \exp\{\mathrm{i}\xi m h\}, \quad v_m^n = \hat{v}^n \exp\{\mathrm{i}\xi m h\},$$
$$U_m^{n,1} = \hat{U}^{n,1} \exp\{\mathrm{i}\xi m h\}, \quad U_m^{n,2} = \hat{U}^{n,2} \exp\{\mathrm{i}\xi m h\}, \text{ etc.},$$

where $\xi \in \mathbb{R}$ and $\mathrm{i} = \sqrt{-1}$. Then, substituting the above expressions into scheme (32) with $V'(U_m^{n,i}) = U_m^{n,i}$, we get

$$\begin{cases} \hat{U}^{n,1} = \hat{u}^n, \\ \hat{U}^{n,2} = \phi_0(\nu_t)\hat{u}^n + \phi_1(\nu_t)\tau\hat{v}^n + \tau^2\phi_2(\nu_t) \left(\omega_t^2 + \dfrac{(e^{\mathrm{i}\xi h} - 2 + e^{-\mathrm{i}\xi h})}{2h^2\phi_2(\nu_x)} - 1 \right) \hat{U}^{n,1}, \\ \hat{u}^{n+1} = \hat{U}^{n,2}, \\ \hat{v}^{n+1} = -\nu_t\omega_t\phi_1(\nu_t)\hat{u}^n + \phi_0(\nu_t)\hat{v}^n \\ \quad + \tau \left(b_1(\nu_t) \Big(\omega_t^2 + \dfrac{(e^{\mathrm{i}\xi h} - 2 + e^{-\mathrm{i}\xi h})}{2h^2\phi_2(\nu_x)} - 1 \Big) \hat{U}^{n,1} + b_2(\nu_t) \Big(\omega_t^2 + \dfrac{(e^{\mathrm{i}\xi h} - 2 + e^{-\mathrm{i}\xi h})}{2h^2\phi_2(\nu_x)} - 1 \Big) \hat{U}^{n,2} \right). \end{cases}$$

Eliminating $\hat{U}^{n,1}$, $\hat{U}^{n,2}$, we obtain

$$\begin{pmatrix} \hat{u}^{n+1} \\ \hat{v}^{n+1} \end{pmatrix} = G \begin{pmatrix} \hat{u}^n \\ \hat{v}^n \end{pmatrix},$$

where

$$G = \begin{pmatrix} 1 - \tau^2\phi_2(\nu_t) + \dfrac{\tau^2\phi_2(\nu_t)\theta}{h^2\phi_2(\nu_x)} & \phi_1(\nu_t)\tau \\ G_{21} & 1 - \tau^2\phi_2(\nu_t) + \dfrac{\tau^2\phi_2(\nu_t)\theta}{h^2\phi_2(\nu_x)} \end{pmatrix},$$

with $\theta = (\cos \xi h - 1)$, and

$$G_{21} = \frac{\tau\phi_1(\nu_t)\theta + \tau^3 b_2(\nu_t)\nu_t^2\phi_2(\nu_t)\theta(\omega_t^2 - 2)}{h^2\phi_2(\nu_x)} + \frac{\tau^3 b_2\phi_2(\nu_t)\theta^2}{h^4\phi_2^2(\nu_x)} - \phi_1(\nu_t)\tau + b_2(\nu_t)\phi_2(\nu_t)\tau^3(1 - \omega_t^2).$$

We can easily verify that $G_{11}G_{22} - G_{12}G_{21} = 1$. Hence, the eigenvalues of $G = G(\xi, \theta, \nu_x, \nu_t)$ satisfy

$$\lambda^2 - (G_{11} + G_{22})\lambda + (G_{11}G_{22} - G_{12}G_{21}) = 0.$$

That is,

$$\lambda^2 - (G_{11} + G_{22})\lambda + 1 = 0. \tag{47}$$

Obviously, the roots λ_i $(i = 1, 2)$ of equation (47) satisfy $|\lambda_i| \leq 1$ if and only if $|G_{11} + G_{22}| \leq 2$. Then the method satisfies the von Neumann condition, which is necessary for the stability [40].

Assuming $|G_{11} + G_{22}| \leq 2$ that

$$\left| 1 - \tau^2\phi_2(\nu_t) + \frac{\tau^2\phi_2(\nu_t)\theta}{h^2\phi_2(\nu_x)} \right| \leq 1,$$

which is equivalent to

$$-1 \leq 1 - \tau^2\phi_2(\nu_t) + \frac{\tau^2\phi_2(\nu_t)\theta}{h^2\phi_2(\nu_x)} \leq 1. \tag{48}$$

Denote $r = \dfrac{\tau}{h}$, and suppose $0 < r \leq \alpha$ and $0 < \nu_t \leq \nu_x \leq \dfrac{\pi}{2}$. Since $\phi_2(\nu)$ is a monotonically decreasing function on the interval $[0, \dfrac{\pi}{2}]$ with $\phi_2(0) = \dfrac{1}{2}$ and $-2 \leq \theta \leq 0$, we obtain

$$\frac{1}{2} - 2\alpha^2\frac{1/2}{\phi_2(\pi/2)} < 1 - \tau^2\phi_2(\nu_t) + \frac{\tau^2\phi_2(\nu_t)\theta}{h^2\phi_2(\nu_x)} < 1.$$

Obviously, if $0 < \alpha \leq \dfrac{\sqrt{6}}{\pi}$, then $\dfrac{1}{2} - 2\alpha^2\dfrac{1/2}{\phi_2(\pi/2)} \geq -1$, and the inequality (48) is satisfied.

Furthermore, it also gives a sufficient condition for the stability of Eleap-frogI. In fact, conditions $0 < \alpha \leq \dfrac{\sqrt{6}}{\pi}$ and $\nu_t \leq \nu_x \leq \dfrac{\pi}{2}$ make $-1 < 1 - \tau^2\phi_2(\nu_t) + \dfrac{\tau^2\phi_2(\nu_t)\theta}{h^2\phi_2(\nu_x)} < 1$, which implies that the equation (47) has two distinct conjugate roots λ_i with $|\lambda_i| = 1$, $i = 1, 2$. Therefore, the method is linearly stable if

$$0 < \alpha \leq \frac{\sqrt{6}}{\pi} \text{ (or equivalently, } 0 < r \leq \frac{\sqrt{6}}{\pi}\text{) and } 0 < \nu_t \leq \nu_x \leq \frac{\pi}{2}.$$

5. Numerical experiments

5.1. The conservation laws and the solution

To investigate the performance of our explicit multi-symplectic schemes, we simulate the evolution of two wave equations as numerical experiments. All computations are done over space region $[-L/2, L/2]$ and we always assume the periodic boundary condition $u(-L/2, t) = u(L/2, t)$ to exclude the boundary effects. The long-time conservation properties of the present schemes are examined by calculating the discrete local/total energy conservation laws.

The local energy conservation law of the Hamiltonian PDE (2) is (5), and for the wave equation (8), we have

$$E(z) = \frac{1}{2}(v^2 + w^2) + V(u), \qquad F(z) = -vw.$$

Integrating (5) over the (m, n)-cell gives

$$\int_{x_m}^{x_{m+1}} \int_{t_n}^{t_{n+1}} (\frac{\partial E}{\partial t} + \frac{\partial F}{\partial x}) dt dx = 0,$$

which implies

$$\int_{x_m}^{x_{m+1}} \left(E\big(z(x, t_{n+1})\big) - E\big(z(x, t_n)\big)\right) dx + \int_{t_n}^{t_{n+1}} \left(F\big(z(x_{m+1}, t)) - F(z(x_m, t)\big)\right) dt = 0. \tag{49}$$

For the MSERKN methods, we approximate the above integral (49) by

$$\begin{aligned}(E_{le})_{mn} = h \sum_{i=1}^{s} \left(\frac{1}{\phi_0(\tilde{c}_i \nu_x)} \left(\tilde{b}_i(\nu_x)\phi_0(\nu_x) + \hat{b}_i(\nu_x)\nu_x^2\phi_1(\nu_x)\right) \right) (E_{m,i}^{n+1} - E_{m,i}^{n}) \\ + \tau \sum_{k=1}^{r} \left(\frac{1}{\phi_0(c_k \nu_t)} \left(b_k(\nu_t)\phi_0(\nu_t) + \bar{b}_k(\nu_t)\nu_t^2\phi_1(\nu_t)\right) \right) (F_{m+1}^{n,k} - F_{m}^{n,k}),\end{aligned}$$

where

$$E_{m,i}^{n} = \frac{1}{2}\left((v_{m,i}^{n})^2 + (w_{m,i}^{n})^2\right) + V(u_{m,i}^{n}), \quad F_{m}^{n,k} = -v_m^{n,k} w_m^{n,k}.$$

We use $(E_{le}^{*})_{mn} = \dfrac{(E_{le})_{mn}}{\tau h}$ to denote the discretization error of the local energy conservation law (5), and $(E_{le})_n = \max_m |(E_{le}^{*})_{mn}|$ to denote the error of the local energy conservation law depending on the time-step.

Then, it can be deduced from (49) that

$$\frac{d}{dt}\varepsilon(t) = \frac{d}{dt} \int_{-L/2}^{L/2} E(x, t) dx = 0,$$

which means that the global energy $\varepsilon(t)$ is a constant. Let the discrete global energy at some fixed time-step t_n be

$$\varepsilon_L^n = h \sum_m \sum_{i=1}^{s} \left(\frac{1}{\phi_0(\tilde{c}_i \nu_x)} \left(\tilde{b}_i(\nu_x)\phi_0(\nu_x) + \hat{b}_i(\nu_x)\nu_x^2\phi_1(\nu_x)\right) \right) E_{m,i}^{n},$$

which is an approximation to the integral

$$\varepsilon(t_n) = \int_{-L/2}^{L/2} E(x, t_n) dx.$$

The error of total energy at time t_n is denoted by $(E_{ge})_n = \varepsilon_L^n - \varepsilon_L^0$, where ε_L^0 is the initial energy.

An example of multi-Hamiltonian PDE is provided by the equation

$$u_{tt} = u_{xx} - \chi \sin u, \tag{50}$$

To show the efficiency and robustness of our new schemes, in our numerical experiments, we use the following schemes:

- leap-frog: the multi-symplectic leap-frog scheme (see [3])

$$\frac{u_m^{n+1} - 2u_m^n + u_m^{n-1}}{\tau^2} = \frac{u_{m+1}^n - 2u_m^n + u_{m-1}^n}{h^2} - V'(u_m^n).$$

- Eleap-frogI: the multi-symplectic scheme Eleap-frogI constructed in Section 4.

- Eleap-frogII: the multi-symplectic scheme Eleap-frogII constructed in Section 4.

We note that these three schemes are explicit, conditionally stable, and of order two in both space and time. We also note that all the three multi-symplectic schemes have the same computational cost with the same step-sizes in time and space.

Since the second order methods Eleap-frogI and Eleap-frogII are the concatenation of two one-stage (or two-stage with FSAL property) symplectic methods, the computational cost of other second order explicit multi-symplectic methods is no less than that of method Eleap-frogI or Eleap-frogII.

Problem 1. We first consider the linear wave equation

$$u_{tt} = u_{xx}, \tag{51}$$

for $\chi = 0$ in (50). The initial conditions employed are

$$u(x,0) = \sin(\pi x),\ \ v(x,0) = -\frac{1}{9}\sin(\pi x).$$

We know that the analytic solution of this problem is

$$u = \sin(\pi x)\cos(\pi t) - \frac{1}{9\pi}\sin(\pi x)\sin(\pi t).$$

Since this problem has oscillations in both space and time, method Eleap-frogI is used to compare with method leap-frog. In the experiment, we chose $\tau = 0.01, h = 0.02, L = 2$, time interval $[0, 20]$, and $\omega_t = \omega_x = \pi$.

Numerical Results:

From Figure 1, it can be seen that Eleap-frogI scheme displays a remarkable superiority over the leap-frog scheme. Both schemes show accumulations of global errors and reasonable oscillation. The accuracy of leap-frog scheme only reaches the magnitude of 10^{-3}, whereas for our scheme Eleap-frogI, the error is about 10^{-14}.

Figure 2 shows the numerical error of local energy conservation law as a function of the time-step calculated by $(E_{le})_n$. As can be seen, the error does not grow with time. The error obtained by leap-frog scheme reaches the magnitude of 10^{-2} and that by Eleap-frogI scheme is about 10^{-3}.

The numerical results related to the variation of the error of the global energy conservation law, i.e., $(E_{ge})_n$, are listed in Figure 3. For both methods, the errors do not show numerical amplifications. Eleap-frogI scheme conserves the global energy perfectly (the scale of 10^{-14}), whereas the leap-frog scheme can only preserve the global energy in the scale of 10^{-3}.

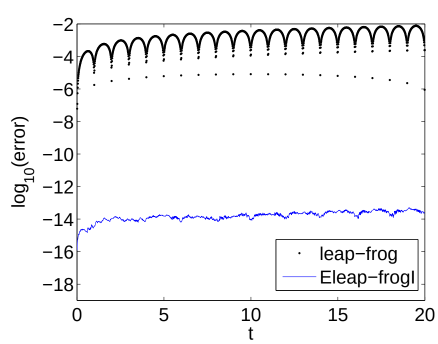

Figure 1: (Problem 1) The logarithm of maximum errors of solution as a function of the time-step.

Problem 2. Let the potential function $V(u)$ in (8) be $V(u) = -\cos(u)$, which gives the well-known sine-Gordon equation with $\chi = 1$ in (50):

$$u_{tt} = u_{xx} - \sin(u).$$

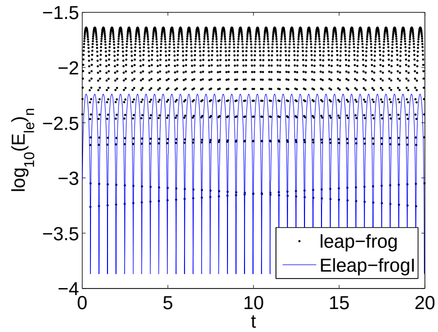

Figure 2: (Problem 1) The logarithm of numerical errors of local energy conservation law as a function of the time-step.

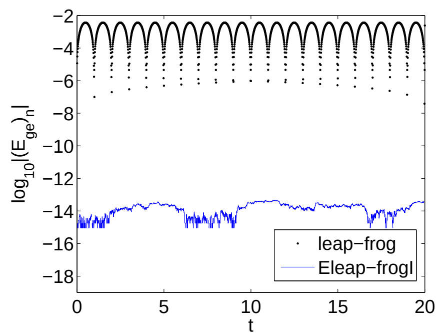

Figure 3: (Problem 1) The logarithm of absolute numerical errors of global energy conservation law as a function of the time-step.

We only consider the so-called breather-solution [11]

$$u(x,t) = 4\tan^{-1}\left(\frac{\sqrt{1-\omega^2}}{\omega}\frac{\cos\omega t}{\cosh(x\sqrt{1-\omega^2})}\right).$$

The initial conditions are given by

$$u(x,0) = 4\tan^{-1}\left(\frac{\sqrt{1-\omega^2}}{\omega}\frac{1}{\cosh(x\sqrt{1-\omega^2})}\right),\ v(x,0) = \frac{\partial}{\partial t}\left\{4\tan^{-1}\left(\frac{\sqrt{1-\omega^2}}{\omega}\frac{\cos\omega t}{\cosh(x\sqrt{1-\omega^2})}\right)\right\}_{t=0},$$

where $\omega = 0.95$. On an infinite domain, this is a bump shaped solution which oscillates up and down with period $2\pi/\omega$. In the experiment, we use $\tau = 0.01$, $h = 0.02$, and time interval $[0, 30]$. To exclude boundary effects, we use period boundary conditions with $L = 80$.

Noticing the exact solution (Figure 7) of the problem, it can be observed that there is only one wave in spatial direction. If we use the Eleap-frogI method, we have to choose $\nu_x = 0$, and then the Eleap-frogI method reduces to the Eleap-frogII method. Thus, we only need to use the Eleap-frogII discretization with fitted frequency $\omega_t = \omega = 0.95$.

Numerical results:

Figure 4 shows the global errors of the two methods. Both schemes display accumulations of global errors and reasonable oscillations. The accuracy of leap-frog scheme reaches the magnitude of 10^{-4} and that of our scheme Eleap-frogII is of 10^{-5}. This is better than classical leap-frog methods.

From Figures 5 and 6, it can be concluded that the scheme Eleap-frogII has a better behavior than the leap-frog scheme in both the error of the local energy conservation law and the global energy conservation law. Here, the difference images between the exact solution and the numerical solutions of the leap-frog and Eleap-frogII schemes are plotted in Figure 8.

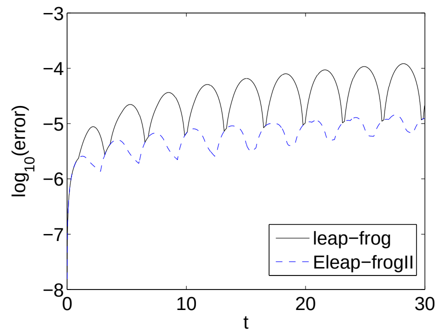

Figure 4: (Problem 2) The logarithm of maximum errors of solution as a function of the time-step.

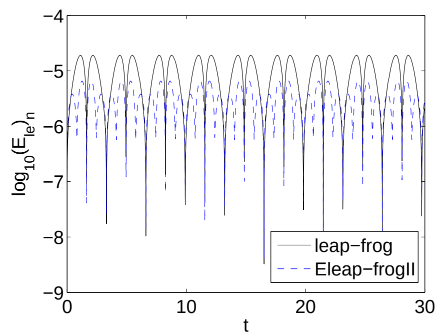

Figure 5: (Problem 2) The logarithm of numerical errors of local energy conservation law as a function of the time-step.

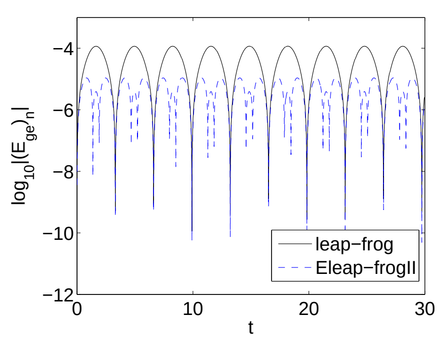

Figure 6: (Problem 2) The logarithm of absolute numerical errors of global energy conservation law as a function of the time-step.

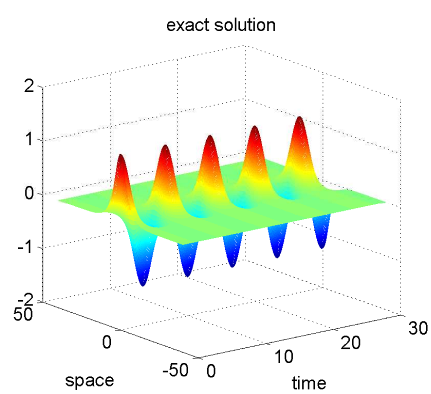

Figure 7: (Problem 2) The exact solution of sine-Gordon equation

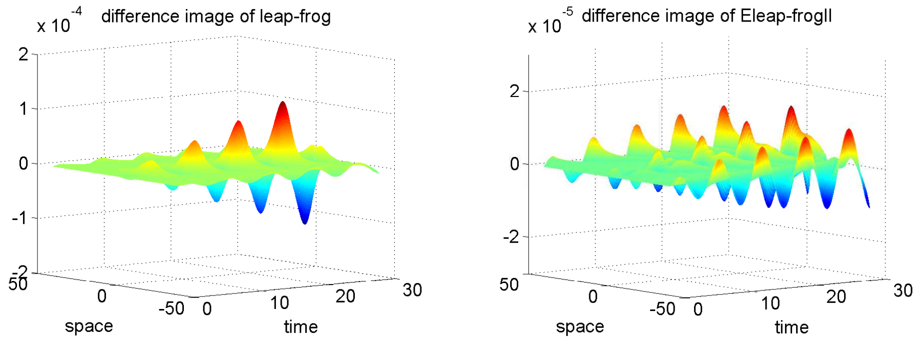

Figure 8: (Problem 2) The difference images between the exact solution and numerical solutions.

It is noted that Hairer and Lubich propose a long-time energy conservation scheme [41]:

$$\begin{cases} y_{n+1} = \cos(h\omega)y_n + \omega^{-1}\sin(h\omega)y_n' + \dfrac{1}{2}h^2\Psi f_n, \\ y_{n+1}' = -\omega\sin(h\omega)y_n + \cos(h\omega)y_n' + \dfrac{1}{2}h(\Psi_0 f_n + \Psi_1 f_{n+1}), \end{cases}$$

where $\Psi = \psi(h\omega)$, $\Phi = \phi(h\omega)$, $\psi(\xi) = \mathrm{sinc}^2(\xi)$, $\phi(\xi) = 1$, $f_n = f(\Phi y_n)$, $\Psi_0 = \psi_0(h\omega)$, and $\Psi_1 = \psi_1(h\omega)$.

Actually, together with the symmetric conditions $\psi(\xi) = \mathrm{sinc}(\xi)\psi_1(\xi)$ and $\psi_0(\xi) = \cos(\xi)\psi_1(\xi)$, this scheme can be regarded as an ERKN method, which can be written in Butcher tableau as follows:

$$\begin{array}{c|cc} 0 & 0 & 0 \\ 1 & \frac{1}{2}\phi_1^2 & 0 \\ \hline \bar{b} & \frac{1}{2}\phi_1^2 & 0 \\ \hline b & \frac{1}{2}\phi_0\phi_1 & \frac{1}{2}\phi_1 \end{array}$$

This scheme is not symplectic in general. However, it is symplectic in the one-dimensional cases, and the concatenation in two directions also deduces a multi-symplectic method. For our experiments, if we use the above scheme instead of the SERKN method (we denote the two schemes as MSHLI and MSHLII, respectively), similar results can be obtained and the numerical effects are very close to those by our new methods constructed in this paper. The results are shown in Tables 1 and 2, where $(E_u)_n = \max_m |u_m^n - \hat{u}_m^n|$ represents the maximum error of the schemes at each time-step t_n, and $\hat{u}_m^n$ denotes the exact solution at (x_m, t_n).

$\tau,\ h$	scheme	$\max_n(E_u)_n$	$\max_n(E_{le})_n$	$\max_n(E_{ge})_n$
$\tau = 0.01,\ h = 0.02$	Eleap-frogI	4.974e − 14	5.741e − 3	4.530e − 14
	MSHLI	1.587e − 13	2.290e − 2	5.156e − 13

Table 1: Numerical results for Problem 1 of schemes Eleap-frogI and MSHLI

$\tau,\ h$	scheme	$\max_n(E_u)_n$	$\max_n(E_{le})_n$	$\max_n(E_{ge})_n$
$\tau = 0.01,\ h = 0.02$	Eleap-frogII	1.442e − 5	6.553e − 6	1.088e − 5
	MSHLII	1.382e − 5	6.720e − 6	1.101e − 5

Table 2: Numerical results for Problem 2 of schemes Eleap-frogII and MSHLII

Moreover, the two schemes MSHLI and MSHLII are also extended leap-frog schemes. Such schemes can be written as:

$$\frac{u_m^{n+1} - \big(2\phi_0(\nu_t) + \nu_t^2\phi_1^2(\nu_t)\big)u_m^n + u_m^{n-1}}{\tau^2\phi_1^2(\nu_t)} = \frac{u_{m+1}^n - \big(2\phi_0(\nu_x) + \nu_x^2\phi_1^2(\nu_x)\big)u_m^n + u_{m-1}^n}{h^2\phi_1^2(\nu_x)} - V'(u_m^n), \qquad (52)$$

with discretizations $w^n_{m+1} = \dfrac{u^n_{m+2} - u^n_m}{2h\phi_1(\nu_x)}, \quad v^{n+1}_m = \dfrac{u^{n+2}_m - u^n_m}{2\tau\phi_1(\nu_t)}$, and

$$\frac{u^{n+1}_m - \big(2\phi_0(\nu_t) + \nu_t^2\phi_1^2(\nu_t)\big)u^n_m + u^{n-1}_m}{\tau^2\phi_1^2(\nu_t)} = \frac{u^n_{m+1} - 2u^n_m + u^n_{m-1}}{h^2} - V'(u^n_m), \tag{53}$$

with discretizations $w^n_{m+1} = \dfrac{u^n_{m+2} - u^n_m}{2h}, \quad v^{n+1}_m = \dfrac{u^{n+2}_m - u^n_m}{2\tau\phi_1(\nu_t)}$, respectively.

5.2. Dispersion analysis

In the study of wave motions, the dispersion relation and group velocity are fundamental concepts (see [42]). A superposition of modes with different wave numbers is wave packet and the dispersion relation gives the relationship between the wave number and the frequency of the modes. Errors in the phase and group velocities lead to the modes traveling with an incorrect speed, which can destroy the qualitative features of the solution [43]. Recent research shows that the multi-symplectic Preissman box scheme, a member of the Gauss-Legendre Runge-Kutta (GLRK) family, qualitatively preserves the dispersion relation of any hyperbolic system (see [44]). Furthermore, for linear PDEs, Frank, et al. [45] shows that the discrete dispersion relation for general s-stage GLRK methods is monotonic and the sign of the analytic group velocity can be preserved. In this subsection, we study the numerical dispersion relation of the schemes Eleap-frogI and Eleap-frogII for linear systems.

From the perspective of integrable nonlinear PDEs, e.g., the sine-Gordon or the KdV equations, the dispersion relation of the associated linearized equation is of importance.

The general oscillatory solution to a linear PDE can be expressed in the form of

$$u(x,t) = \int_{-\infty}^{\infty} A(k)e^{\mathrm{i}\left(kx-\omega(k)t\right)}\,dk, \tag{54}$$

where k, $\omega(k)$, and $A(k)$ are the wave number, wave frequency, and amplitude, respectively, and $Ae^{\mathrm{i}(kx-\omega t)}$ itself is a solution of the linear PDE. The wave number k and frequency $\omega(k)$ are related by the following dispersion relation [45]:

$$D(\omega,k) = 0 \Leftrightarrow \omega = \omega(k),$$

which is uniquely determined by the specified PDE and is used to characterize the system. For example, the linearization

$$u_{tt} - u_{xx} + \chi u = 0 \tag{55}$$

of the sine-Gordon equation (50) at $u = 0$ has a dispersion relation

$$D(\omega,k) = \omega^2 - k^2 - \chi = 0. \tag{56}$$

The phase velocity is defined by $v_p(k) = \omega/k$. In a non-dispersive system, such as the wave equation (51), every wave has the same phase velocity ($v_p = c_0$) and the solution for $t > 0$ is just the initial condition translated through space: $u(x,t) = u(x - c_0t, 0)$.

An important quantity of dispersive systems is the group velocity defined by, $v_g(k) = \omega'(k) = -\dfrac{\partial D}{\partial k}\Big/\dfrac{\partial D}{\partial \omega}$. The group velocity is usually a function of the wave number k and characterizes the speed of energy transport in wave packets. In this case, $\omega''(k) \neq 0$, and waves with different wave numbers travel with different phase velocities v_p, which brings the group velocity dispersion (GVD) and ultimately causes the spatial spreading of the wave packet.

The dispersive properties of the discretizations can be studied by calculating their numerical dispersion relations. To do so, we start with the discretizations of the linearized sine-Gordon equation (55) associated with the Eleap-frogI and Eleap-frogII schemes in their single equation format

$$\begin{cases} \text{Eleap}-\text{frogI}: \dfrac{D_t^2u^{n-1}_m}{2\phi_2(\nu_t)} - \dfrac{D_x^2u^n_{m-1}}{2\phi_2(\nu_x)} + \chi u^n_m = 0, \\ \text{Eleap}-\text{frogII}: \dfrac{D_t^2u^{n-1}_m}{2\phi_2(\nu_t)} - D_x^2u^n_{m-1} + \chi u^n_m = 0, \end{cases} \tag{57}$$

where $D_t u_m^n = \dfrac{u_m^{n+1} - u_m^n}{\tau}$ and $D_x u_m^n = \dfrac{u_{m+1}^n - u_m^n}{h}$ are the finite difference operators.

Assume a discrete general solution to a linear PDE of the form $\sum_K Ae^{\mathrm{i}(Km-\Omega n)}$, $K = kh$, $\Omega = \omega\tau$, where each mode is a solution provided K and Ω satisfy a numerical dispersion relation

$$D_N(\Omega, K) = 0.$$

For the equation (57), the corresponding numerical dispersion relations are given by

$$\begin{cases} \text{Eleap}-\text{frogI}: \left(\dfrac{\sqrt{2\phi_2(\nu_t)}}{\phi_2(\nu_t)\tau}\sin\dfrac{\Omega}{2}\right)^2 - \left(\dfrac{\sqrt{2\phi_2(\nu_x)}}{\phi_2(\nu_x)h}\sin\dfrac{K}{2}\right)^2 - \chi = 0, \\ \text{Eleap}-\text{frogII}: \left(\dfrac{\sqrt{2\phi_2(\nu_t)}}{\phi_2(\nu_t)\tau}\sin\dfrac{\Omega}{2}\right)^2 - \left(\dfrac{2}{h}\sin\dfrac{K}{2}\right)^2 - \chi = 0. \end{cases} \tag{58}$$

Both these two schemes preserve the form of the analytical dispersion relation (56). The exact relationship is given by the following theorem.

Theorem 5.1. *The multi-symplectic schemes* (58) *qualitatively preserves the dispersion relation of the linear PDE. Specifically, there exist diffeomorphisms ψ_1 and ψ_2 satisfying the exact dispersion relationship*

$$D_N(\Omega, K) = D\big(\psi_1(\Omega), \psi_2(K)\big) = \psi_1^2 - \psi_2^2 - \chi = 0, \tag{59}$$

where

$$\begin{cases} \text{Eleap}-\text{frogI}: \big(\psi_1(\Omega), \psi_2(K)\big) = \left(\dfrac{\sqrt{2\phi_2(\nu_t)}}{\phi_2(\nu_t)\tau}\sin\dfrac{\Omega}{2}, \dfrac{\sqrt{2\phi_2(\nu_x)}}{\phi_2(\nu_x)h}\sin\dfrac{K}{2}\right), \\ \text{Eleap}-\text{frogII}: \big(\psi_1(\Omega), \psi_2(K)\big) = \left(\dfrac{\sqrt{2\phi_2(\nu_t)}}{\phi_2(\nu_t)\tau}\sin\dfrac{\Omega}{2}, \dfrac{2}{h}\sin\dfrac{K}{2}\right), \end{cases} \tag{60}$$

for $-\pi < K, \Omega < \pi$.

Solving the numerical dispersion relations (58) gives

$$\begin{cases} \text{Eleap}-\text{frogI}: \Omega(K) = \pm 2\arcsin\sqrt{\dfrac{\phi_2(\nu_t)r^2}{\phi_2(\nu_x)}\sin^2\dfrac{K}{2} + \dfrac{\phi_2(\nu_t)hr}{2}\chi}, \\ \text{Eleap}-\text{frogII}: \Omega(K) = \pm 2\arcsin\sqrt{2\phi_2(\nu_t)r^2\sin^2\dfrac{K}{2} + \dfrac{\phi_2(\nu_t)hr}{2}\chi}. \end{cases}$$

The significance of Theorem 5.1 for the non-dispersive equation (55) (with $\chi = 0$) can be seen in Figures 9–11, which show the dispersion curves $\Omega(K)$, the group velocity $\Omega^{'}(K)$, the group velocity dispersion $\Omega^{''}(K)$ for the exact (56), and numerical (58). In the experiment, two different values of the ratio $r = \tau/h$, with $h = 0.01$ are used. The exact relation is given by $\Omega(K) = \pm rK$.

The significance of Theorem 5.1 for the linearized sine-Gordon equation (55) (with $\chi = 1$) can be seen in Figures 12–14. The exact relation is given by $\Omega(K) = \pm r\sqrt{K^2 + h^2}$.

From Figures 9–14, we can see that the existence of diffeomorphisms (60) is not enough to preserve the qualitative features of the analytical solution. All of the schemes introduce numerical dispersions. From Figures 10 and 13, because $\Omega(K)$ and K both have direction, we can see that the dispersion relation curves are all monotonically increasing at rates given by their numerical group velocities. Similarly, Figures 11 and 14 display that the group velocity curves (see Figures 10 and 13) are monotonically decreasing. Therefore, considering the numerical solutions of the linear wave equations given by Eleap-frogI and Eleap-frogII schemes, we further obtain the following corollaries.

Corollary 5.1. *The numerical group velocities $V_g(k) = \Omega^{'}(K) = -\dfrac{\partial D_N}{\partial K}\Big/\dfrac{\partial D_N}{\partial \Omega}$ at (K, Ω) of the two schemes Eleap-frogI and Eleap-frogII have the same sign as the group velocity $v_g(k) = \omega^{'}(k) = -\dfrac{\partial D}{\partial k}\Big/\dfrac{\partial D}{\partial \omega}$ for the associated pair (k, ω).*

Corollary 5.2. *Both Eleap-frogI and Eleap-frogII schemes introduce negative dispersion, and when the wave number is increasing, the numerical group velocities are monotonically decreasing.*

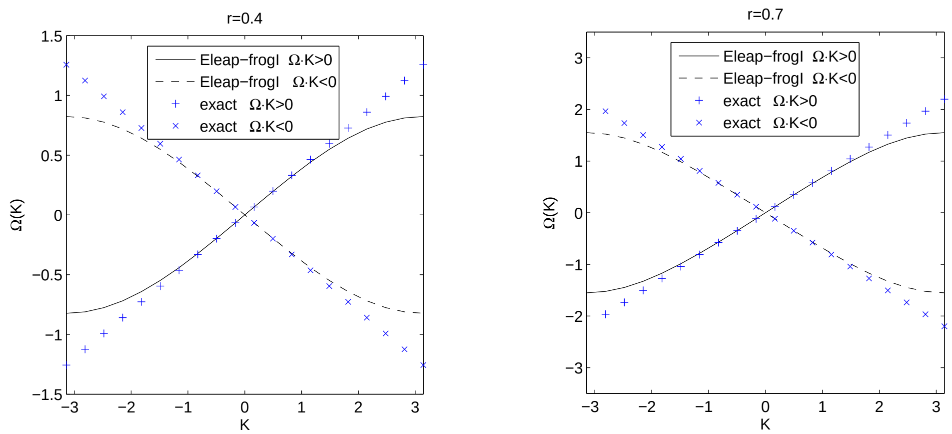

Figure 9: Dispersion relations curves for the scheme Eleap-frogI for the linear wave equation $u_{tt} = u_{xx}$.

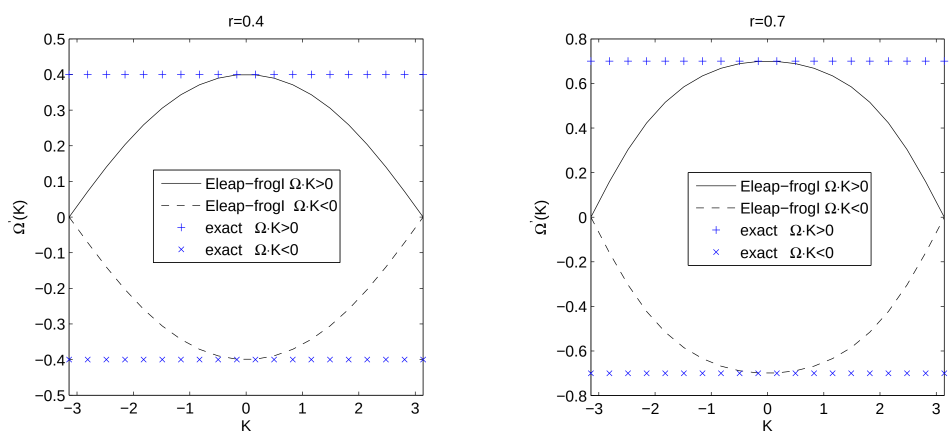

Figure 10: Group velocities curves for the scheme Eleap-frogI for the linear wave equation $u_{tt} = u_{xx}$.

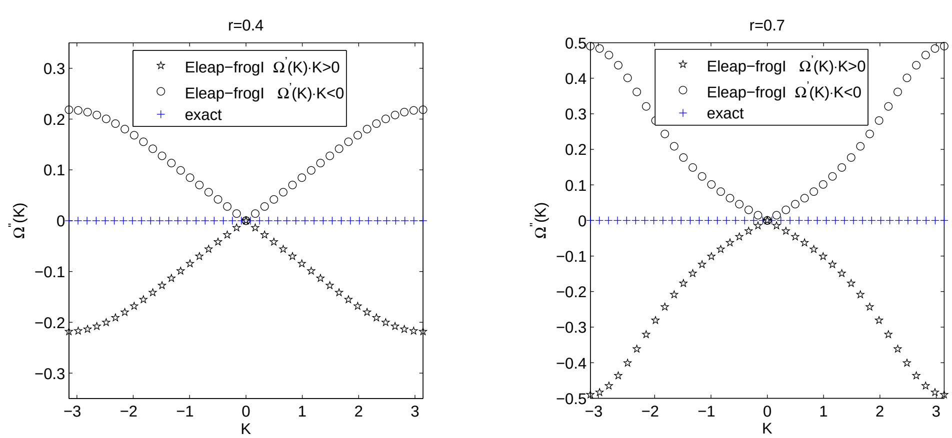

Figure 11: Group velocities dispersion curves for the scheme Eleap-frogI for the linear wave equation $u_{tt} = u_{xx}$.

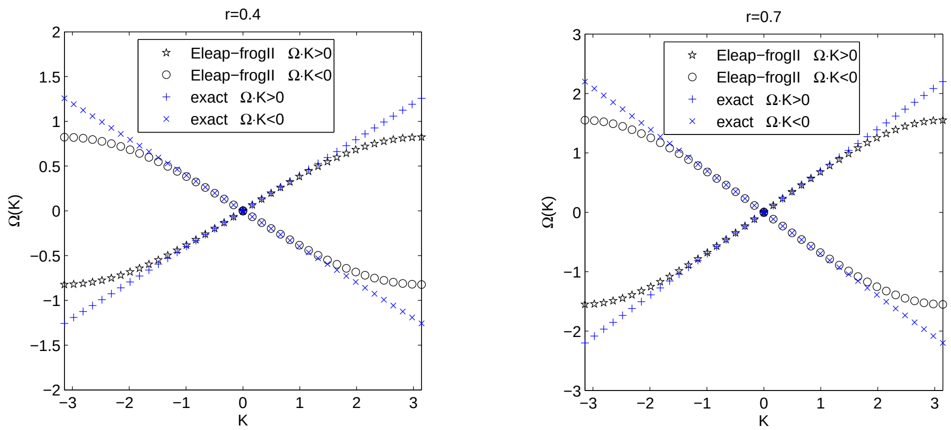

Figure 12: Dispersion relations curves for the scheme Eleap-frogII for the linearized sine-Gordon equation.

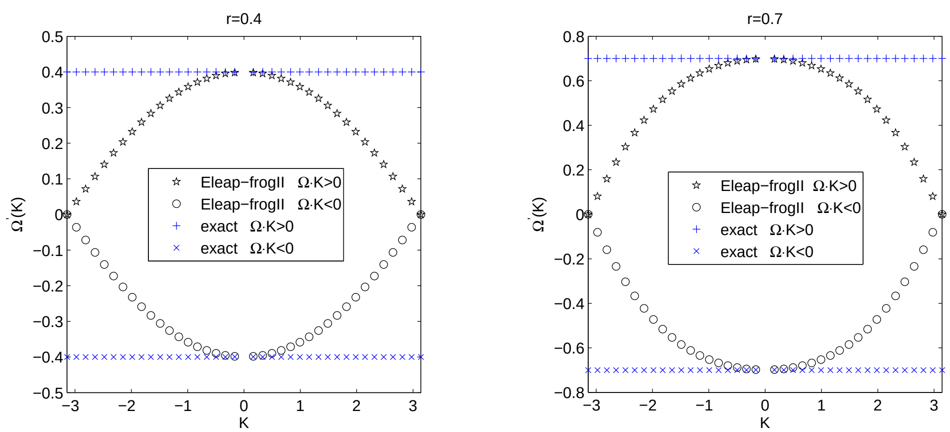

Figure 13: Group velocities curves for the scheme Eleap-frogII for the linearized sine-Gordon equation.

6. Conclusion

In this paper, we discuss the issue of applying multi-symplectic extended Runge-Kutta-Nyström methods to Hamiltonian wave equations, and investigate the conservative properties of the methods. Two new explicit multi-symplectic integrators Eleap-frogI and Eleap-frogII are proposed. The numerical conservation laws and the solutions are accompanied by applying the two new methods and the well-known leap-frog method to the linear wave equation and the sine-Gordon equation. We also discuss the dispersion relations of the new schemes. Numerical results illustrate the robustness of the new explicit multi-symplectic integrators. We believe that more efficient multi-symplectic integrators can be constructed, since it allows more types of methods for concatenation.

Acknowledgements

We greatly appreciate the anonymous referees for reading carefully the manuscript and for providing valuable suggestions which help improve significantly the presentation of the paper.

References

[1] E. Hairer, C. Lubich, and G. Wanner, Geometric Numerical Integration: Structure-Preserving Algorithms, Springer-Verlag, Berlin, Heidelberg, 2002.

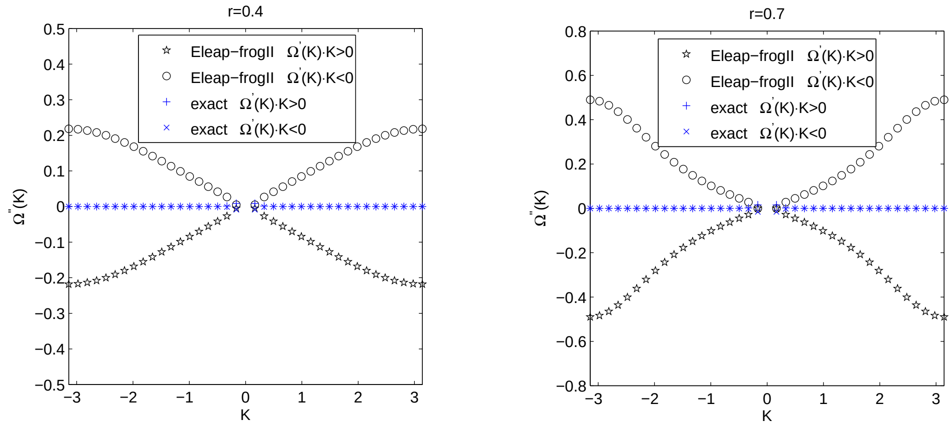

Figure 14: Group velocities dispersion curves for the scheme Eleap-frogII for the linearized sine-Gordon equation.

[2] T. J. Bridges, A geometric formulation of the conservation of wave action and its implications for signature and the classification of instabilities, Proc. Roy. Soc. London Ser. A 453 (1997) 1365–1395.

[3] T. J. Bridges, and S. Reich, Multi-symplectic integrators: Numerical schemes for Hamiltonian PDEs that conserve symplecticity, Phys. Lett. A 284 (2001) 184–193.

[4] J. E. Marsden, G. P. Patric, and S. Shkoller, Multi-symplectic geometry, variational integrators, and nonlinear PDEs, Comm. Math. Phys. 4 (1999) 351–395.

[5] J. Hong, A survey of multi-symplectic Runge-Kutta type methods for Hamiltonlian partial differential equations, in: T. Li and P. Zhang (Eds.), Frontiers and Prospects of Contemporary Applied Mathematics, Series in Contemporary Applied Mathematics, Higher Education Press,Word Scientific Beijing, 6 (2005) 71–113.

[6] J. Hong, and C. Li, Multi-symplectic Runge-Kutta methods for nonlinear Dirac equations, J. Comput. Phys. 211 (2006) 448–472.

[7] J. Hong, H. Liu, and G. Sun, The multi-symplecticity of partitioned Runge-Kutta methods for Hamiltonian PDEs, Math. Comput. 75 (2006) 167–181.

[8] J. Hong, S. Jiang, C. Li, and H. Liu, Explicit multi-symplectic methods for Hamiltonian wave equation, Comm. Comput. Phys. 2 (2007) 662–683.

[9] H. Liu, and K. Zhang, Multi-symplectic Runge-Kutta-type methods for Hamiltonian wave equations, IMA J. Numer. Anal. 26 (2006) 252–271.

[10] Q. Li, Y. Song, and Y. Wang, On multi-symplectic partitioned Runge-Kutta methods for Hamiltonian wave equations, Appl. Math. Comput. 177 (2006) 36–43.

[11] S. Reich, Multi-symplectic Runge-Kutta collcation methods for Hamiltonian wave equations, J. Comput. Phys. 157 (2000) 473–499.

[12] B. N. Ryland, and R. I. Mclachlan, On Multisymplectic of Partitioned Runge-Kutta Methods. SIAM J. Sci. Comput. 30 (2008) 1318–1340.

[13] J. M. Franco, Runge-Kutta-Nyström methods adapted to the numerical integration of perturbed oscillators, Comput. Phys. Comm. 147 (2002) 770–787.

[14] X. Wu, X. You, and J. Li, Note on derivation of order conditions for ARKN methods for perturbed oscillators, Comput. Phys. Comm., 180 (2009) 1545–1549.

[15] X. Wu, X. You, and J. Xia, Order conditions for ARKN methods solving oscillatory systems, Comput. Phys. Comm., 180 (2009) 2250–2257.

[16] W. Shi, and X. Wu, On symplectic and symmetric ARKN methods, Comput. Phys. Comm. 183 (2012) 1250–1258.

[17] X. Wu, A note on stability of multidimensional adapted Runge-Kutta-Nyström methods for oscillatory systems, Appl. Math. Modell.,doi.org/10.1016/j.apm.2012.01.053.

[18] H. Yang, X. Wu, X. You, and Y. Fang, Extended RKN-type methods for numerical integration of perturbed oscillators, Comput. Phys. Comm. 180 (2009) 1777–1794.

[19] X. Wu, X. You, W. Shi, and B. Wang, ERKN integrators for systems of oscillatory second-order differential equations, Comput. Phys. Comm. 181 (2010) 1873–1887.

[20] X. Wu, B. Wang, and J. Xia, Explicit symplectic multidimensional exponential fitting modified Runge-Kutta-Nyström methods, BIT Numer. Math. DOI 10.1007/s10543-012-0379-z (2012).

[21] X. Wu, B. Wang, K. Liu, and H. Zhao, ERKN methods for long-term integration of multidimensional orbital problems Appl. Math. Modell., doi.org/10.1016/j.apm.2012.05.021.

[22] L.Gr. Ixaru, and G. Vanden Bergehe (Eds), Exponential Fitting, Kluwer Academic Publishers, Dordrecht, 2004.

[23] Y. Fang, and X. Wu, A trigonometrically fitted explicit Numerov-type method for second-order initial value problems with oscillating solutions, Appl. Numer. Math., 58 (2008), 341–351.

[24] H. Yang, and X. Wu, Trigonometrically-fitted ARKN methods for perturbed oscillators, Appl. Numer. Math., 58 (2008), 1375–1395.

[25] Y. Fang, Y. Song, and X. Wu, Trigonometrically fitted explicit Numerov-type method for periodic IVPs with two frequencies, Comput. Phys. Comm., 179 (2008), 801–811.

[26] T. Monovasilis, and T.E. Simos, New second-order exponentially and trigonometrically fitted symplectic integrators for the numerical solution of the time-independent Schrödinger equation, J. Math. Chem, 42 (2007) 535–545.

[27] T. E. Simos, Closed Newton-Cotes Trigonometrically-Fitted Formulae of High-Order for Long-Time Integration of Orbital Problems, Appl. Math. Lett. 22 (2009) 1616–1621.

[28] T. E. Simos, Closed Newton-Cotes Trigonometrically-Fitted Formulae for the Solution of the Schrödinger Equation, MATCH Commun. Math. Comput. Chem. 60 (2008) 787–801.

[29] T. E. Simos, Closed Newton-Cotes trigonometrically-fitted formulae of high order for the numerical integration of the Schrödinger equation, J. Math. Chem. 44 (2008) 483–499.

[30] T. E. Simos, High-order closed Newton-Cotes trigonometrically-fitted formulae for long-time integration of orbital problems, Comput. Phys. Commun. 178 (2008) 199–207.

[31] T. Monovasilis, Z. Kalogiratou, and T.E. Simos, Computation of the eigenvalues of the Schrödinger equation by symplectic and trigonometrically fitted symplectic partitioned Runge-Kutta methods, Phys. Lett. A 372 (2008) 569–573.

[32] Z. Kalogiratou, Th. Monovasilis, and T.E. Simos, New modified Runge-Kutta-Nyström methods for the numerical integration of the Schrödinger equation, Comput. Math. Appl. 60 (2010) 1639–1647.

[33] A. B. González, P. Martín, and J. M. Farto, A new family of Runge-Kutta type methods for the numerical integration of perturbed oscillators, Numer. Math. 82 (1999) 635–646.

[34] T. J. Bridges, Multi-symplectic structures and wave propagation, Math. Proc. Camb. Phil. Soc. 121 (1997) 147–190.

[35] R. I. McLachlan, Symplectic integration of Hamiltonian wave equations, Numer. Math. 66 (1994) 465–492.

[36] K. W. Morton and D. F. Mayers, Numerical Solution of Partial Differential Equations, Cambridge University Press, 2005.

[37] X. Wu, B. Wang, and J. Xia, Extended symplectic Runge-Kutta-Nyström integrators for separable Hamiltonian systems, in Proceedings of the 2010 International Conference on Computational and Mathematical Methods in Science and Engineering, Vol. III (Editor J. Vigo Aguiar), Spain, (2010) 1016–1020.

[38] E. Hairer, S. P. Nøsett, and G. Wanner, Solving Ordinary Differential Equation I: Nonstiff Problems, Second Edition, Springer-Verlag, Berlin, Heidelberg, 1993.

[39] Y. B. Suris, On the canonicity of mappings that can be generated by methods of Runge-Kutta type for integrating systerms $x'' = -\frac{\partial U}{\partial x}$, in Russian, Zh. Vychisl. Mat. Fiz. 29 (1989), 202–211; U.S.S.R. Comput. Math. and Math. Phys. (translation), 29 (1990) 138–144.

[40] A. Iserles, A First Course in the Numerical Analysis of Differential Equations, Cambridge University Press, Cambridge, 1996.

[41] E. Hairer, and C. Lubich, Long-Time Energy Conservation of Numerical Methods for Oscillatory Differential Equations, SIAM Journal on Numerical Analysis, Vol. 38, No. 2 (2001) 414–441.

[42] C. M. Schober, and T. H. Wlodarczyk, Dispersive properties of multi-symplectic integrators, J. Comput. Phys. 227 (2008) 5090–5104.

[43] L. N. Trefethen, Group velocities in finite difference schemes, SIAM Rev. 24 (1982) 113–136.

[44] U. M. Asher and R. I. McLachlan, Multisymplectic box scheme and the Kortweg-de Vries equation, Appl. Numer. Math. 48 (2004) 255–269.

[45] J. Frank, B. E. Moore, and S. Reich, Linear PDEs and numerical methods that preserve a multisymplectic conservation law, SIAM J. Sci. Comput. 28 (2006) 260–277.